JAERI-M
82-151

# EVALUATION OF NEUTRON CROSS SECTIONS FOR VANADIUM

October 1982

Shigeya TANAKA

日本原子力研究所
Japan Atomic Energy Research Institute

JAERI-Mレポートは，日本原子力研究所が不定期に公刊している研究報告書です。
入手の問合わせは，日本原子力研究所技術情報部情報資料課（〒319-11茨城県那珂郡東海村）あて，お申しこしください。なお，このほかに財団法人原子力弘済会資料センター（〒319-11茨城県那珂郡東海村日本原子力研究所内）で複写による実費頒布をおこなっております。

JAERI-M reports are issued irregularly.
Inquiries about availability of the reports should be addressed to Information Section, Division of Technical Information, Japan Atomic Energy Research Institute, Tokai-mura, Naka-gun, Ibaraki-ken 319-11, Japan.



編集兼発行　日本原子力研究所
印　　刷　㈱高野高速印刷

JAERI-M 82-151

# Evaluation of Neutron Cross Sections for Vanadium

Shigeya TANAKA

Division of Physics,
Tokai Research Establishment, JAERI

(Received October 5, 1982)

Comprehensive neutron nuclear data for vanadium have been evaluated from thermal region to 20 MeV, and the results are to be filed in the ENDF/B format as an elemental component in Japanese Evaluated Nuclear Data Library-Version 2 (JENDL-2). The data base, the evaluation procedure and judgement, and the final results are described. The results include the neutron total cross sections, all significant partial cross sections of neutron induced reactions and the resonance parameters of vanadium. Particular attention has been payed to higher energy processes having an impact on FBR and CTR.

Keywords: Evaluation, Vanadium, Neutron Nuclear Data, Total Cross Section, Partial Cross Sections, Resonance Parameters, JENDLE-2, Optical-Model, Statistical Model

---

The work was performed within the activities of Japanese Nuclear Data Committee.

# バナジウムの中性子断面積評価

日本原子力研究所東海研究所物理部

田中　茂也

（１９８２年１０月５日受理）

熱エネルギー領域から２０MeVの範囲におけるバナジウムの核データ評価を行った。その結果はENDF／Bフォーマットの形で，わが国の評価ずみ核データライブラリー第２版（JENDL－２）に収録されることになっている。この論文には，評価に用いたデータベース，評価手続きとその判定，および評価結果が述べられている。その内容としては，バナジウムの中性子全面積，無視できるものを除いたすべての部分断面積，および共鳴パラメータが含まれている。高速炉および核融合炉ニュートロニックスへの利用を考えて，特に高いエネルギー領域における評価に注意が払われている。

この仕事はシグマ研究委員会の活動の下で行われた。

Contents

# 目　　次

## 1. Introduction

Comprehensive evaluated neutron nuclear data for vanadium are presented. The data base, the evaluation procedure and judgement, and the final results are described in the present paper. The energy range of the evaluated data covers thermal region to 20 MeV. The present work was submitted to Nuclear Data Center in JAERI as an elemental component of JENDL-2.

Vanadium is thought to be a promissing structural material for use in high temperature neutronic system, in particular, where tritium is a concern. Therefore, although the present evaluation is comprehensive, particular attention has been payed rather to high energy processes which have an impact on FBR and CTR.

Natural vanadium consists mainly of $^{51}V$ (its isotropic abundance is 99.76 %). Hence, in practical application, it may be sufficient that only $^{51}V$ is considered, except for a resonance peak contribution from $^{50}V$ in the lower energy region.

Experimental cross section data on the elastic and inelastic scattering, the $(n,\gamma)$ reaction and the threshold reactions are not always available in the energy region higher than several MeV. Hence, theoretical calculations based on the optical model and the statistical model have to be employed in order to obtain evaluated cross sections. The author has reported that the coupled-channel calculations with one set of optical parameters can well reproduce the total and scattering cross sections over a wide energy and mass region[1]. It is not easy, however, to perform the coupled-channel calculation for $^{51}V$, because the application of the weak coupling between vibrational core and $j = 7/2$ proton for this nucleus does not lead to good results[2]. For convenience' sake, the spherical optical-model calculations are employed in the present work.

The energy range covered by the present work is divided into three regions; (1) resonance region up to 100 keV, (2) unresolved resonance region from 100 to 500 keV and (3) continuum region higher than 500 keV. The evaluation procedure for the continuum region rather depends on the model calculation. The experimental data used in the evaluation have mostly been taken from NEUDADA File, whose data were received from NEA Data Bank at Saclay. The data were retrieved by the computer codes NESTOR[3] and REPSTOR[4].

## 2. Resonance Region (up to 100 keV)

The resonance parameters for $^{51}V$ are listed in Table 1. The total, elastic and $(n,\gamma)$ reaction cross sections can be calculated with these parameters.

These parameters were obtained by modifying some values in $^{51}V$ resonance parameters from BNL 325 (3rd Edition)[6] so that the results calculated with the multi-level Breit-Wigner (MLBW) formula reproduced well mainly the experimental total cross sections. The fitting procedure was repeated several times by means of the try-and-error method with NDES Code[5], which employed an interactive CTR display system.

In the calculation, levels between $10^{-5}$ eV and 153 keV were considered, and parameter values, which were not given in BNL 325 (3rd Edition), were assumed as follows:

$\ell = 1$ for weak levels,

$\ell = 0$ for levels at 118.5,134.5, 140.9, 145.6 and 152.7 keV[7],

$J = 3.5$, where J is the spin value of a resonance level,

$\Gamma_\gamma = 0.5$ eV, where $\Gamma_\gamma$ is the radiative width.

Contribution from ten levels, to which the neutron width $\Gamma_n$ had not been assigned, were neglected. For all of these levels, $\ell = 1$ and $2g\Gamma_n\Gamma_\gamma/\Gamma = 0.4$

The energy range covered by the present work is divided into three regions; (1) resonance region up to 100 keV, (2) unresolved resonance region from 100 to 500 keV and (3) continuum region higher than 500 keV. The evaluation procedure for the continuum region rather depends on the model calculation. The experimental data used in the evaluation have mostly been taken from NEUDADA File, whose data were received from NEA Data Bank at Saclay. The data were retrieved by the computer codes NESTOR[3] and REPSTOR[4].

## 2. Resonance Region (up to 100 keV)

The resonance parameters for $^{51}V$ are listed in Table 1. The total, elastic and $(n,\gamma)$ reaction cross sections can be calculated with these parameters.

These parameters were obtained by modifying some values in $^{51}V$ resonance parameters from BNL 325 (3rd Edition)[6] so that the results calculated with the multi-level Breit-Wigner (MLBW) formula reproduced well mainly the experimental total cross sections. The fitting procedure was repeated several times by means of the try-and-error method with NDES Code[5], which employed an interactive CTR display system.

In the calculation, levels between $10^{-5}$ eV and 153 keV were considered, and parameter values, which were not given in BNL 325 (3rd Edition), were assumed as follows:

$\ell = 1$ for weak levels,

$\ell = 0$ for levels at 118.5,134.5, 140.9, 145.6 and 152.7 keV[7],

$J = 3.5$, where J is the spin value of a resonance level,

$\Gamma_\gamma = 0.5$ eV, where $\Gamma_\gamma$ is the radiative width.

Contribution from ten levels, to which the neutron width $\Gamma_n$ had not been assigned, were neglected. For all of these levels, $\ell = 1$ and $2g\Gamma_n\Gamma_\gamma/\Gamma = 0.4$

eV are assigned in BNL 325 (3rd Edition) and no prominent peaks at energies for these levels appear on the measured cross section data. Here, g is the statistical weight factor and $\Gamma = \Gamma_n + \Gamma_\gamma$. For the potential scattering radius, R' = 5 fm was taken. In the calculation, the Doppler broadening effect was not considered.

The calculated total cross sections are compared with measured values in Figs. 1.1 - 1.4. In the figures solid lines represent the calculated results. Agreement is not always good over the whole energy region. The recommended values are to be corrected for addition of point-wise background cross sections shown in Table 2 to the calculated cross sections. In Fig. 1.1 symbol " + " and dotted line represent the data of Palevsky[8] and those of Bendt[9], respectively. The present calculation shows smaller values than those data. In Figs. 1.2 and 1.3, dotted lines up to 26 keV represent the data of Firk et al.[10] In the energy region higher than 20 keV, the data of Rohr and Friedland[7] are available, and they are shown by a dashed line. The data of Firk et al. show poor agreement with those of Rohr and Friedland in the energy range of 20 - 26 eV. Here, we adopted the values of Rohr and Friedland in the energy region higher than 20 keV. In addition to those data, there are data of Cotè et al.[11] in the energy region 3.2 to 90 keV and data of Amram et al.[12] in the region 0.58 to 580 keV. However, the former data are coarse in energy steps and the latter generally give lower peak values than those of Firk et al. and those of Rohr and Friedland.

The $(n,\gamma)$ cross section calculated from the resonance parameters is indicated by a solid line in Fig. 2 in the energy range $10^{-3}$ eV to 20 keV. (The result in the range 20 to 100 keV is omitted from the graphic presentation because of its complicate feature.) The dotted line shows the ENDF/B-IV evaluated data[13]. A peak at 0.167 keV observed by Kapchigashev[14] (open

circles in Fig. 2) is due to $^{50}V$ (abundance 0.24 %) in natural vanadium. Disagreement of the solid line with this peak and with experimental values below 1 keV are to be corrected by means of background cross sections shown in Table 2.

The elastic scattering cross sections in the resonance region are obtained by subtracting the (n,$\gamma$) reaction cross sections from the total cross sections.

## 3. Unresolved Resonance Region (100 to 500 keV)

The total and (n,$\gamma$) reaction cross sections are main concern in the unresolved resonance region. The channel of the inelastic scattering cross section for the first excited level opens at $E_n$ = 320.1 keV, and its contribution should be taken into account, though it is not large.

### 3.1 Total Cross Section

The evaluated total cross section shown by thick solid lines in Figs. 3.1 and 3.2 was obtained based on the experimental data. In the energy range 100 to 220 keV, the data of Rohr and Friedland[7] (thin solid line in Fig. 3.1) were roughly followed for the evaluation. In the energy range from 220 to 360 keV, only the data of Smith et al.[15] (dotted line in Figs.3.1 and 3.2) are reasonably good resolution data. The fluctuation patterns of these data, however, appear on the several keV higher side of energy than those of Rohr and Friedland in the energy region 100 to 220 keV, and show the same tendency in the region 360 to 500 keV compared with the high resolution data of Cierjacks et al.[16] (thin solid line in Fig. 3.2). Therefore, in the energy range 220 to 360 keV, the evaluated values were lowered several keV for the data of Smith et al. Above 360 keV, the evaluated values follow

circles in Fig. 2) is due to $^{50}V$ (abundance 0.24 %) in natural vanadium. Disagreement of the solid line with this peak and with experimental values below 1 keV are to be corrected by means of background cross sections shown in Table 2.

The elastic scattering cross sections in the resonance region are obtained by subtracting the (n,$\gamma$) reaction cross sections from the total cross sections.

## 3. Unresolved Resonance Region (100 to 500 keV)

The total and (n,$\gamma$) reaction cross sections are main concern in the unresolved resonance region. The channel of the inelastic scattering cross section for the first excited level opens at $E_n$ = 320.1 keV, and its contribution should be taken into account, though it is not large.

### 3.1 Total Cross Section

The evaluated total cross section shown by thick solid lines in Figs. 3.1 and 3.2 was obtained based on the experimental data. In the energy range 100 to 220 keV, the data of Rohr and Friedland[7] (thin solid line in Fig. 3.1) were roughly followed for the evaluation. In the energy range from 220 to 360 keV, only the data of Smith et al.[15] (dotted line in Figs.3.1 and 3.2) are reasonably good resolution data. The fluctuation patterns of these data, however, appear on the several keV higher side of energy than those of Rohr and Friedland in the energy region 100 to 220 keV, and show the same tendency in the region 360 to 500 keV compared with the high resolution data of Cierjacks et al.[16] (thin solid line in Fig. 3.2). Therefore, in the energy range 220 to 360 keV, the evaluated values were lowered several keV for the data of Smith et al. Above 360 keV, the evaluated values follow

the data of Cierjacks et al. Their data agree well with the data of Smith et al. except for the systematic energy deviation just mentioned. There are also data of Blair[17] (shown by open circles) and of Cabé et al.[18] (shown by triangles) abailable. If one considers the inferior resolution of those data, it may be said that the data of Cierjacks et al. agree well with those data.

### 3.2 (n,γ) Reaction

The evaluated (n,γ) reaction cross section was obtained also based on experimental data. In the energy range up to 210 keV, the recent fine resolution data of Winters et al.[19] are available. The evaluation followed roughly those data. Table 3 gives the (n,γ) data together with the total cross section data adopted in the present work. In the energy range 210 to 500 keV, the evaluation (solid line in Fig. 4) followed the data of Dudey et al.[20] (shown by ⊖ in Fig. 4).

### 3.3 Inelastic Scattering to the First Excited Level

The evaluated inelastic scattering cross sections are given by Hauser-Feshbach[21] calculations, which will be mentioned in the next section. The calculated result for the inelastic scattering cross section for the first excited level was filed in the form of point-wise data as the evaluation in the unresolved resonance region.

### 3.4 Elastic Scattering

The elastic scattering cross section $\sigma_{el}$ in the energy range 100 to 500 keV is obtained by

$$\sigma_{el} = \sigma_T - \sigma_{n,\gamma} - \sigma_{inel},$$

where $\sigma_T$ is the total cross section, $\sigma_{n,\gamma}$ the (n,$\gamma$) reaction cross section, and $\sigma_{inel}$ the inelastic scattering cross section for the first excited level. The angular distributions of the elastic scattering may be assumed to be isotropic.

## 4. Continuum Region (above 0.5 MeV)

The evaluated data of the elastic, major part of inelastic and total cross sections in the continuum region are given by model calculations using the computer codes ELIESE-3[22] and CASTHY[23]. The following partial cross sections were evaluated based on the experimental data or cited from other evaluations:

(i) Inelastic scattering cross sections for the first and second excited levels in the energy region higher than 4.5 MeV,

(ii) the threshold reaction cross sections such as (n,2n), (n,n'p), (n,$\alpha$), (n,p), (n,d), (n,t), (n,n'$\alpha$) reactions.

### 4.1 Model Parameters

The spherical optical model was used to obtain potential parameters. The experimental total and elastic scattering cross sections were fitted by the calculations. As to the starting values of the potential parameters, the same parameter set as employed in the previously reported coupled-channel calculations[1] was taken, and by considering the difference between the spherical and collective models, the potential depth of the imaginary part W and the nuclear radius parameter $r_0$ (nuclear radius is given by $R = r_0 A^{1/3}$) were changed as follows:

$W = 2.55\ E^{1/2}$ ---------> $W = 4.6 + 0.34\ E$ (MeV),

$r_0 = 1.25$ ---------> $r_0 = 1.23$ (fm).

where $\sigma_T$ is the total cross section, $\sigma_{n,\gamma}$ the (n,γ) reaction cross section, and $\sigma_{inel}$ the inelastic scattering cross section for the first excited level. The angular distributions of the elastic scattering may be assumed to be isotropic.

## 4. Continuum Region (above 0.5 MeV)

The evaluated data of the elastic, major part of inelastic and total cross sections in the continuum region are given by model calculations using the computer codes ELIESE-3[22] and CASTHY[23]. The following partial cross sections were evaluated based on the experimental data or cited from other evaluations:

(i) Inelastic scattering cross sections for the first and second excited levels in the energy region higher than 4.5 MeV,

(ii) the threshold reaction cross sections such as (n,2n), (n,n'p), (n,α), (n,p), (n,d), (n,t), (n,n'α) reactions.

### 4.1 Model Parameters

The spherical optical model was used to obtain potential parameters. The experimental total and elastic scattering cross sections were fitted by the calculations. As to the starting values of the potential parameters, the same parameter set as employed in the previously reported coupled-channel calculations[1] was taken, and by considering the difference between the spherical and collective models, the potential depth of the imaginary part W and the nuclear radius parameter $r_0$ (nuclear radius is given by $R = r_0 A^{1/3}$) were changed as follows:

$W = 2.55\ E^{1/2}$ ---------> $W = 4.6 + 0.34\ E$ (MeV),

$r_0 = 1.25$ ---------> $r_0 = 1.23$ (fm).

The rest of parameter values are given by

$$V = 51.85 - 0.33\,E - 24.0\,(N - Z)/A \quad \text{(MeV)},$$

$$a = 0.65 \quad \text{(fm)},$$

$$V_{so} = 7.0 \quad \text{(MeV)},$$

$$b = 0.48 \quad \text{(fm)},$$

where V and $V_{so}$ are the potential depths of the real part and the spin-orbit coupling term, respectively, and a and b the diffuseness parameters of the real part and imaginary part, respectively. For the imaginary potential, the derivative Woods-Saxon form was used.

Calculated results are shown in the following. The solid line in Fig. 5 shows the result of the total cross section. Averaged experimental data are represented by various symbols. Good fit to the experimental data was obtained above 400 keV. The calculated cross sections fit to the data within 7 % in the energy region from 400 keV to 4 MeV, and within 2 % above 4 MeV.

Fairly good overall fit was obtained also for the differential elastic scattering cross sections above several hundred keV. Features of the fitness are shown in Figs. 6.1 - 6.3. In the calculation, the contribution of the compound-elastic scattering was considered for the cross sections up to a neutron energy 3.6 MeV. Calculations for the compound process will be mentioned below. As seen in Fig. 6.1, agreement of the calculated results with the measured values is rather poor. The measured cross sections show prominent fluctuation in the region lower than MeV[15]. A comparison of the calculated result with averaged cross sections was tryed. The hatched area shows the range of uncertainty of the cross sections averaged over an energy interval of (403 $\pm$ 100) keV. The agreement is a little improved, but disagreement still remains in the forward direction. Hence, use of the present optical potential for the Hauser-Feshbach calculations might lead to

results with some ambiguity, especially for cross sections near thresholds.

In the calculation of the Hauser-Fshbach formula, 26 levels up to 3.674 MeV including the ground level were taken into account. The level parameters [24] are shown in Table 4. Above 3.678 MeV, levels were considered to overlap. For the levels with unknown spin-parities, arbitrary values were assumed. These are shown by brackets [ ] in Table 4 to make difference from assigned values.

As for the level density parameters, those given by Dilg et al.[25] were adopted, because rather good results were obtained with their parameters in the present work. According to the method of Dilg et al., they used the Fermi-gas model, but did not use the constant-temperature model for nuclei even in the region of low excitation energy. Instead, in their method fictitive ground state was back-shifted relative to the conventionally shifted ground state as determined by the pairling energy. Their level density parameter a and energy shift $\Delta$ for $^{51}V$ are 6.39 $MeV^{-1}$ and 0.21 MeV, respectively. For $^{52}V$, Dilg et al. gave a = 5.59 $MeV^{-1}$ and $\Delta$ = -2.38 MeV. In the present work, the value of a was adjusted from 5.59 $MeV^{-1}$ to 5.97 $MeV^{-1}$. To calculate the spectrum of the (n,2n) reaction, a and for $^{50}V$ are needed. As these were not given by Dilg. et al., they were assumed as the same as those of $^{52}V$ in the present work.

In the Hauser-Feshbach calculations, competing process such as the $(n,\gamma)$ reaction and the threshold reactions were taken into consideration. For the latter effect, the present evaluation of the threshold reaction cross sections was used as the input of computer calculations using the code CASTHY. The $(n,\gamma)$ branching was calculated within the code CASTHY. Parameters of the giant resonance level used in the $(n,\gamma)$ calculation were $E_R$ = 18.0 MeV, $\Gamma_R$ = 5.0 MeV and y = 0.5 with the Brink-Axel type[26] of the profile function, where $E_R$ is the resonance energy, $\Gamma_R$ the reso-

nance width and y the fraction of exchange forces[27].

## 4.2 Total Cross Section

As was mentioned above, the evaluated cross section above 0.5 MeV is given by the optical model calculation.

## 4.3 Elastic Scattering

The evaluated elastic scattering cross section in the energy range 0.5 to 4.5 MeV is given by the model calculation. Above 4.5 MeV, the integrated elastic scattering cross section $\sigma_{el}$ should be decreased by the same amount as the sum of corrections added to the inelastic scattering cross sections for the first and second excited levels in order to keep the sum rule, $\sigma_T = \sum_i \sigma_i$, where $\sigma_T$ is the total cross section and $\sigma_i$ a partial cross section. The reason for the corrections for the inelastic scattering cross sections is mentioned in Subsection 4.4. The angular distributions of the inelastic scattering can be estimated by the model calculations normalized to $\sigma_{el}$.

## 4.4 Inelastic Scattering

The evaluated inelastic scattering cross sections are given by the Hauser-Feshbach calculation, except for those for two low-lying levels. The reason for the exception is as follows. In the present work the direct reaction was not calculated. As a convention, experimental data of Perey and Kinney[28] were roughly followed from 4.5 to 8.5 MeV (see Figs. 7.1 and 7.2). This means that in the present evaluation some artificial corrections were added to the Hauser-Feshbach calculations. As there are no experimental data available above 8.5 MeV, the same values of the corrections at 8.5 MeV

were added also to the calculations in the energy range above 8.5 MeV.

As seen in Figs. 7.1 - 7.4, there are large discrepancies among the experimental data. Therefore, it is hard to make rigorous discussions about the validity of the present evaluation.

### 4.5 (n,γ) Reaction

The evaluated (n,γ) reaction cross section above 0.5 MeV is given by the model calculation using the code CASTHY. The result of the calculation is shown in Fig. 4 up to 2.4 MeV. In the calculation, the cross section was normalized to 3.0 mb at 0.4 MeV so as to be smoothly connected to the evaluated value at 0.5 MeV. The calculated result follows the data of Dudey et al.[20] Above 2.4 MeV, there are some data available at 14 MeV. Present evaluation gives a little smaller value than those data.

### 4.6 (n,2n) Reaction

As shown in Fig. 8, only two sets of experimental data are available for the V(n,2n) reaction. Frehaut et al.[29] have reported measured values in the energy range 11.4 to 14.8 MeV. On the other hand, Ashby et al.[30] have given 660 mb to the cross section at 14.1 MeV. As shown in Fig. 8, this is about 100 mb as large as the interpolation of the values of Frehaut et al. Ashby et al. have given also a fairly large value for the Cu(n,2n) reaction cross section compared with other measurements. Therefore, the present evaluated curve is given based on the values of Frehaut et al. Above 15 MeV, the curve is an extrapolation guided by experimental data of $^{63}$Cu(n,2n) reaction. The neutron spectrum is given by the model calculation normalized to the present evaluation by using the code CASTHY.

4.7 (n,p) Reaction

As shown in Fig. 9, almost all measurements were made around 14 MeV using the activation technique. Only Bormann et al.[31] have given several data points in the energy range 13 to 18 MeV. Their data around 14 MeV come quite close to the average of other author' data. There are no data available in the range lower than 13 MeV. The present evaluation, therefore, adopts the result calculated by Kitazawa and Isogai[32], who have normalized their result to the data of Bormann et al. at 13.2 MeV. Their calculation was made based on the evaporation model and Blann's hybrid model[33]. In the calculation, Becchetti, Jr. and Greelees' (B-G) parameters[34] were employed for the optical potential, and Blann's nuclear radius and Fermi energy of 40 MeV were used for the latter model. The $Vr^2$ value[35] of the B-G parameter set is very close to that of the present optical parameters (68.4 and 68.0 MeV at $E_n$ = 14 MeV, respectively), but it is difficult to compare the effect of the imaginary part. The use of present parameter set might give a little different (n,p) reaction cross sections.

4.8 (n,n'p) Reaction

Robertson et al.[37] and Grimes et al.[38] have given 87 mb at 14 MeV and 91 $\pm$ 14 mb at 15 MeV for the $^{51}$V(n,xp) reaction cross section, respectively. Major part of this reaction may be the (n,p) and (n,n'p) reactions. These values, however, seem to be too large. The evaluated values were given by subtracting the evaluated (n,p) reaction cross section from the result calculated by Kitazawa and Isogai for the $^{51}$V(n,xp) reaction cross section[32]. In the calculation, the absolute value for the (n,xp) reaction cross section were fixed relative to the calculated values for the (n,p) reaction cross section.

4.9 (n,d) Reaction

The measurement for the $^{51}V(n,d)^{50}V$ reaction cross section is to observe outgoing deuterons. The activation method is not applicable for the reason that $^{50}Ti$ is a stable nudeus. Ilakovac et al.[39] have given 6 mb to the (n,d) reaction cross section for the excited states of $^{50}Ti$ up to third level at an energy of 14.4 MeV. Grimes et al.[38] have reported 7 ± 3 mb for the (n,d) reaction cross section at 15 MeV. The evaluated curve was obtained by normalizing the relative values of the excitation function calculated by Guenther et al.[36] to the value of Grimes et al.

4.10 (n,t) Reaction

Khurana and Govil[40] have suggested that the cross section for the $^{51}V(n,t)$ reaction may be in the order of 1 mb at 14 MeV. As a convention, the evaluation followed roughly the shape of the (n,d) reaction cross section with a normalization value of 1 mb at 14 MeV.

4.11 (n,α) Reaction

As shown in Fig. 10, although there are many experimental data for $^{51}V(n,\alpha)$ reaction, large scatter is seen among the data sets of the energy-dependent measurements as well as the data points around 14 MeV. However, if the data published before 1964 are discarded and if the $^{51}V(n,x\alpha)$ reaction cross sections recently measured by Robertson et al.[37] and Grimes et al.[38] are included assuming that the major contribution to the reaction comes from the (n,α) reaction, then the average value of the data around 14 MeV amounts to a value very close to the data of Paulsen et al.[41] The present evaluation, therefore, follows their data points.

4.12 (n,n'α) Reaction

Bormann et al.[42] measured the $^{51}V(n,n'\alpha)$ reaction cross section in the energy range 13 to 20 MeV by the activation technique. They obtained the cross section by observing 160 keV gamma rays from $^{49}Sc$, but Hillman [43] asserted that they could not discriminate 175 keV gamma rays originated from the $^{51}V(n,\alpha)^{48}Sc$ reaction. He mentioned that the $^{51}V(n,n'\alpha)$ reaction cross section would be less than 0.3 mb at 14 MeV. Here, the author would like to support Hillman's assertion.

5. Summary

Neutron nuclear data for vanadium have been evaluated in the energy range of thermal to 20 MeV. It was divided into three regions; (1) resonance region ( up to 100 keV), (2) unresolved resonance region (100 to 500 keV), and (3) continuum region (500 keV to 20 MeV).

For the resonance region , the resonance parameters were obtained by modifying some values in those from BNL 325 (3rd Edition)[6], so that the result calculated with the MLBW formula could well reproduce the observed total cross sections. Agreement was not always good over the whole energy region. There was a tendency that the calculated total cross sections gave lower values in the electron volt region and higher values in the region above several tens of keV than the experimental values. Therefore, the addition of artificial background cross sections were needed.

The evaluated total and (n,γ) reaction cross sections in the unresolved resonance region were obtained based on the experimental data. The measured structures were incorporated into the file. The features of these structures are shown in Figs. 3.1, 3.2 and 4, and also in Fig. 11.

4.12 (n,n'α) Reaction

Bormann et al.[42] measured the $^{51}V(n,n'\alpha)$ reaction cross section in the energy range 13 to 20 MeV by the activation technique. They obtained the cross section by observing 160 keV gamma rays from $^{49}Sc$, but Hillman [43] asserted that they could not discriminate 175 keV gamma rays originated from the $^{51}V(n,\alpha)^{48}Sc$ reaction. He mentioned that the $^{51}V(n,n'\alpha)$ reaction cross section would be less than 0.3 mb at 14 MeV. Here, the author would like to support Hillman's assertion.

5. Summary

Neutron nuclear data for vanadium have been evaluated in the energy range of thermal to 20 MeV. It was divided into three regions; (1) resonance region ( up to 100 keV), (2) unresolved resonance region (100 to 500 keV), and (3) continuum region (500 keV to 20 MeV).

For the resonance region , the resonance parameters were obtained by modifying some values in those from BNL 325 (3rd Edition)[6], so that the result calculated with the MLBW formula could well reproduce the observed total cross sections. Agreement was not always good over the whole energy region. There was a tendency that the calculated total cross sections gave lower values in the electron volt region and higher values in the region above several tens of keV than the experimental values. Therefore, the addition of artificial background cross sections were needed.

The evaluated total and (n,γ) reaction cross sections in the unresolved resonance region were obtained based on the experimental data. The measured structures were incorporated into the file. The features of these structures are shown in Figs. 3.1, 3.2 and 4, and also in Fig. 11.

The spherical optical model and the statistical model were used to estimate the total and elastic scattering cross sections above 0.5 MeV, the major part of the inelastic scattering cross sections and the $(n,\gamma)$ reaction cross section. Starting from the parameter set in ref. 1), the potential depth of the imaginary part and the radius parameter were altered to $W = 4.6 + 0.36\ E$ (MeV) and $r_0 = 1.23$ (fm), respectively, so that the calculated total and differential elastic scattering cross sections could be fitted to the experimental data. Fairly good fit was obtained for the total and elastic scattering cross sections above several hundred keV. However, care must be taken in the case of application of the present potential to the calculation of the cross section at the energy lower than several hundred keV. The cross sections for the threshold reactions were evaluated based on the experimental data, the calculations done by Kitazawa and Isogai and ENDF/B-IV evaluation for $(n,n'\alpha)$ reaction.

Fig. 11 shows a log-log plot for the present evaluation in the unresolved resonance and continuum regions. The $(n,\gamma)$ reaction cross sections were not drawn in the fogure, because most of them are less than 10 mb, except for several resonance peaks. The $(n,n'\alpha)$ reaction cross section does not appear there, because it is less than 10 mb.

Note added: The resonance data in BNL-325 4th Edition were not able to be used in this work, because the book was published after most of the resonance analyses in the present work had been completed.

References

1) Tanaka, S.: JAERI-M 5984, p. 212 (1975)

2) Funsten, H.O., Robertson, N.R. and Rost, E.: Phys. Rev. 134, B117 (1964)

3) Nakagawa,T.: to be published

4) Nakagawa, T.: to be published

5) Nakagawa, T.: JAERTI-M 8163, p. 51 (1979) and to be published

6) BNL-325, 3rd Edition,Vol. 1 (1973) editted by Mughabgab, S. and Garber, D.

7) Rohr, G. and Friedland, E.: Nucl. Phys. A104, 1 (1967)

8) Palevsky, H.: data from NEUDADA (1953)

9) Bendt, P.J.: data from NEUDADA (1953)

10) Firk, R.W.K., Lynn, J.E. and Moxon, M.C.: Proc. Phys. Soc. 82, 477 (1963)

11) Coté, R.E., Bollinger, L.M. and LeBlanc, J.M.: Phys. Rev. 111, 288 (1958)

12) Amram, Y., Huynh, V.D., Julien, J., Morgenstern, J. and Netter, F.: Bul. Am. Phys. Soc. 7, 288 (1962)

13) ENDF/B-IV data file for vanadium (MAT 1196) evaluated by Penny, S.K. and Owen, L.W., (ENDF-201) editted by Garber, G., available from NNDC, BNL, Upton, N. Y. (Oct., 1975)

14) Kapchigashev, S.P.: Atomnaya Energ. 19, 294 (1965)

15) Smith, A.B., Whalen, J.F. and Takeuchi, K.: Phys. Rev. C1, 581 (1970)

16) Cierjacks, S., Forti, P., Kopsch, L., Nebe, J. and Unseld, H.: KFK 1000 (1968)

17) Blair, J.: Phys. Rev. 79, 28 (1950)

18) Cabé, J., Laurat, M., Yvon, P. and Bardolle, G.: Nucl. Phys. A102, 92 (1967)

19) Winters, R.R., Macklin, R.L. and Halperin, J.: Phys. Rev. C18, 2092 (1978)

20) Dudey, N.D., Heinrich, R.R. and Madson, A.A.: Jour. Nucl. Energ. 23, 443 (1969)

21) Hauser, W. and Feshbach, H.: Phys. Rev. 87, 366 (1952)

22) Igarasi, S.: JAERI 1224 (1972)

23) Igarasi, S.: to be published

24) Auble, R.L.: Nucl. Data Sheets 23, 163 (1978)

25) Dilg, W., Schantl, W., Vonach, H. and Uhl, M.: Nucl. Phys. A217, 269 (1973)

26) Axel, P.: Phys. Rev. 126, 672 (1962)

27) Lane, A.M. and Lynn, J.E.: Nucl. Phys. 11, 646 (1959)

28) Perey, F. and Kinney, W.: ORNL-4551 (1970)

29) Frehaut, J. et al.: from EXFOR 2057.003 (1976)

30) Ashby, V.J., Carton, H.C., Newkirk, L.L. and Taylor, C.J.: Phys. Rev. 111, 616 (1958)

31) Borman, M., Cierjacks, S., Fretwurst, E., Giesecke, K.J., Neuert, H. and Pollehn, H.: Zeit. Phys. 174, 1 (1963)

32) Kitazawa, H. and Isogai, Y.: Private communication

33) Blann, M.: Nucl. Phys. A213, 570 (1973)

34) Becchetti, Jr., F.D. and Greenlees, G.W.: Phys. Rev. 182, 1190 (1969)

35) e.g. Hodgson, P.E., in Nuclear Reaction and Nuclear Structure (Clarendon Press, Oxford, 1971) p. 156

36) Guenther, P., Havel, D. Howerton,R., Mann, F., Smith, D., Smith, A. and Whalen, J.: ANL/NDM-24 (1977)

37) Robertson, J.C., Andric, B. and Kolkowski, P.: Jour. Nucl. Energ. 27, 531 (1973)

38) Grimes, S.M., Haight, R.C. and Anderson, J.D.: Phys. Rev. C17, 508 (1978)

39) Ilakovac, K., Kuo, L.G., Petravic, M., Slaus, I., Tomas, P. and Satchler, G.R.: Phys. Rev. 128, 2739 (1962)

40) Khurana, C. and Govil, I.: Nucl. Phys. 69, 153 (1965)

41) Paulsen, A., Widera, R. and Liskien, H: Atomkernenergie 22, 291 (1973)

42) Bormann, M., Cierjacks, S., Langkau, R. and Neuert, H.: Zeit. Phys. 166, 477 (1962)

43) Hillman, M.: Phys. Rev. 129, 2227 (1963)

44) Towle, J.H.: Nucl. Phys. A117, 657 (1968)

45) Holmqvist, B. and Wiedling, T.: Nucl. Phys. A146, 321 (1970)

46) Ferrer, J.C., Carlson, J.D. and Rapaport, J.: Nucl. Phys. A275, 325 (1977)

I =7/2$^-$ *

Table 1 Resonance Parameters of $^{51}V$

| $E_0$ (keV) | J | ℓ | $\Gamma_n$ (eV) | $\Gamma_\gamma$ (eV) |
|---|---|---|---|---|
| 4.20 | 4 | 0 | 470 | 1.32 |
| 6.95 | 3 | 0 | 1000 | 2.45 |
| 11.75 | 3 | 0 | 4500 | 1.87 |
| 16.23 | 4 | 0 | 344 | 1.50 |
| 21.70 | 3 | 0 | 725.7 | 1.50 |
| 29.63 | 4 | 0 | 160 | 0.5 |
| 39.44 | 3 | 0 | 537.1 | 0.98 |
| 48.04 | 4 | 0 | 115.6 | (1.0) |
| 49.50 | 3 | 0 | 560 | (1.0) |
| 51.90 | 4 | 0 | 88 | (1.0) |
| 52.97 | 3 | 0 | 500 | (1.0) |
| 63.10 | 3 | 0 | 3200 | (1.0) |
| 68.60 | 4 | 0 | 3900 | (1.0) |
| 73.50 | (3.5) | 0 | 30 | (1.0) |
| 82.60 | 4 | 0 | 700 | (1.0) |
| 87.30 | 4 | 0 | 1800 | (1.0) |
| 110.3 | (3.5) | 0 | 250 | (1.0) |
| 116.0 | 4 | 0 | 240 | (1.0) |
| 118.5 | 4 | (0) | 18500 | (1.0) |
| 118.5 | (3.5) | 0 | 140 | (0.5) |
| 134.5 | 4 | (0) | 2700 | (0.5) |
| 140.9 | 3 | (0) | 2700 | (0.5) |
| 145.6 | 3 | (0) | 1200 | (0.5) |
| 152.7 | 4 | (0) | 3502 | (0.5) |
| 16.99 | (3.5) | (1) | 310 | (0.5) |
| 29.9 | 3 | 1 | 3.43 | 0.53 |
| 33.51 | 2 | 1 | 22.4 | 0.5 |
| 37.43 | 4 | 1 | 21.33 | 0.55 |
| 40.9 | 5 | 1 | 4.36 | 1.2 |
| 42.37 | 4 | 1 | 21.33 | 0.57 |
| 44.45 | (3.5) | 1 | 8.0 | (0.5) |
| 45.9 | 2 | 1 | 16 | 0.56 |
| 48.4 | (3.5) | (1) | 15 | (0.5) |
| 78.7 | (3.5) | (1) | 20 | (0.5) |
| 83.7 | (3.5) | (1) | 160 | (0.5) |
| 92.9 | (3.5) | (1) | 70 | (0.5) |
| 94.5 | (3.5) | (1) | 74 | (0.5) |
| 95.3 | (3.5) | (1) | 50 | (0.5) |
| 96.8 | (3.5) | (1) | 24 | (0.5) |
| 98.3 | (3.5) | (1) | 50 | (0.5) |
| 103.5 | (3.5) | (1) | 24 | (0.5) |
| 114.2 | (3.5) | (1) | 70 | (0.5) |
| 127.4 | (3.5) | (1) | 70 | (0.5) |

Values with parentheses are those assumed in the calculation.

* The spin-parity value of the target nucleus.

Table 2 Background Cross Sections ($B_i$) in the Resonance Region

| $E_n$ (eV) | $B_\gamma$ (b) | $B_{el}$ (b) | $B_T$ (b) |
|---|---|---|---|
| 0.001 | 4.0 | given by $B_T - B_\gamma$ | 7.0 |
| 0.01 | 2.0 | | 4.0 |
| 0.1 | 0.4 | | 1.5 |
| 1.0 | 0.2 | | 1.1 |
| 10 | 0.05 | | 0.8 |
| 100 | 0.02 | | 0.5 |
| 120 | (0.015) | | (0.5) |
| 150 | (0.04) | | (0.5) |
| 167 | (0.97) | | (0.97) |
| 180 | (0.016) | | (0.5) |
| 1000 | 0.008 | | 0.5 |
| 4300 | 0 | 0.5 | 0.5 |
| 5000 | 0 | 14.0 | 14.0 |
| 6000 | 0 | 0 | 0 |
| 6800 | 0 | -30.0 | -30.0 |
| 7000 | 0 | 0 | 0 |
| 7600 | 0 | 0 | 0 |
| 7700 | 0 | -15 | -15 |
| 8200 | 0 | -15 | -15 |
| 9500 | 0 | 0 | 0 |
| 72000 | 0 | 0 | 0 |
| 77000 | 0 | -15 | -15 |
| 100000 | 0 | -15 | -15 |

The value with parentheses should be used only for natural vanadium. The background cross section between the given $E_n$ values is obtained by log-log interpolation for $E_n < 100$ eV, and by linear interpolation for $E_n > 100$eV. The background cross section lower than 0.001 eV is given by 1/v-law down to $10^{-5}$ eV.

Table 3 Data in the Region 100 to 210 keV Adopted in the Present Evaluation

| $E_n$ (keV) | $\sigma_T$ (b) | $\sigma_{n\gamma}$ (b) |
|---|---|---|
| 100 | 1.0 | .0057 |
| 105 | 1.7 | .004 |
| 110 | 4.0 | .008 |
| 112 | 7.0 | .005 |
| 119 | 13.0 | .016 |
| 124 | 13.0 | .009 |
| 130 | 7.0 | .005 |
| 132 | 0.8 | .006 |
| 136 | 11.6 | .013 |
| 139 | 8.4 | .007 |
| 141 | 11.2 | .012 |
| 144 | 2.2 | .003 |
| 145 | 9.0 | .011 |
| 148 | 2.3 | .003 |
| 150 | 0.5 | .003 |
| 153 | 9.0 | .014 |
| 158 | 2.2 | .004 |
| 160 | 12.2 | .015 |
| 168 | 9.8 | .007 |
| 170 | 3.0 | .006 |
| 174 | 6.4 | .006 |
| 180 | 7.9 | .010 |
| 184.5 | 12.5 | .0075 |
| 187 | 4.5 | .019 |
| 189 | 14.0 | .007 |
| 198 | 2.6 | .005 |
| 210 | 7.9 | .012 |
| 204 | 11.2 | .006 |
| 210 | 4.8 | .005 |

Table 4 Discrete-Level Parameters of $^{51}V$

LEVEL PARAMETERS

| NO | ENERGY | SPIN | PARITY | NO | ENERGY | SPIN | PARITY | NO | ENERGY | SPIN | PARITY |
|---|---|---|---|---|---|---|---|---|---|---|---|
| 0 | 0.0 | 3.5 | - | 1 | 0.32000 | 2.5 | - | 2 | 0.92900 | 1.5 | - |
| 3 | 1.60900 | 5.5 | - | 4 | 1.81300 | 4.5 | - | 5 | 2.40900 | 1.5 | - |
| 6 | 2.54500 | 0.5 | + | 7 | 2.67500 | 1.5 | + | 8 | 2.69900 | 7.5 | - |
| 9 | 2.79000 | [4.5 | - ] | 10 | 3.08400 | (2.5) | - | 11 | 3.19500 | [2.5 | - ] |
| 12 | 3.21500 | (1.5) | - | 13 | 3.26200 | (2.5 | - ) | 14 | 3.28000 | (2.5) | [ + ] |
| 15 | 3.38100 | (1.5 | - ) | 16 | 3.38300 | (4.5 | - ) | 17 | 3.38600 | (6.5 | - ) |
| 18 | 3.39600 | (6.5 | - ) | 19 | 3.41200 | [4.5 | - ] | 20 | 3.45200 | (4.5 | - ) |
| 21 | 3.51500 | [6.5 | - ] | 22 | 3.56900 | [6.5 | - ] | 23 | 3.57600 | [1.5 | - ] |
| 24 | 3.61400 | (5.5 | - ) | 25 | 3.63100 | [0.5 | - ] | 26 | 3.67400 | (1.5 | - ) |

LEVELS ABOVE 3.680 MEV ARE ASSUMED TO BE OVERLAPPING

( ): Weak assignments cited from the original evaluation,

[ ]: Arbitrary assignments in the present work.

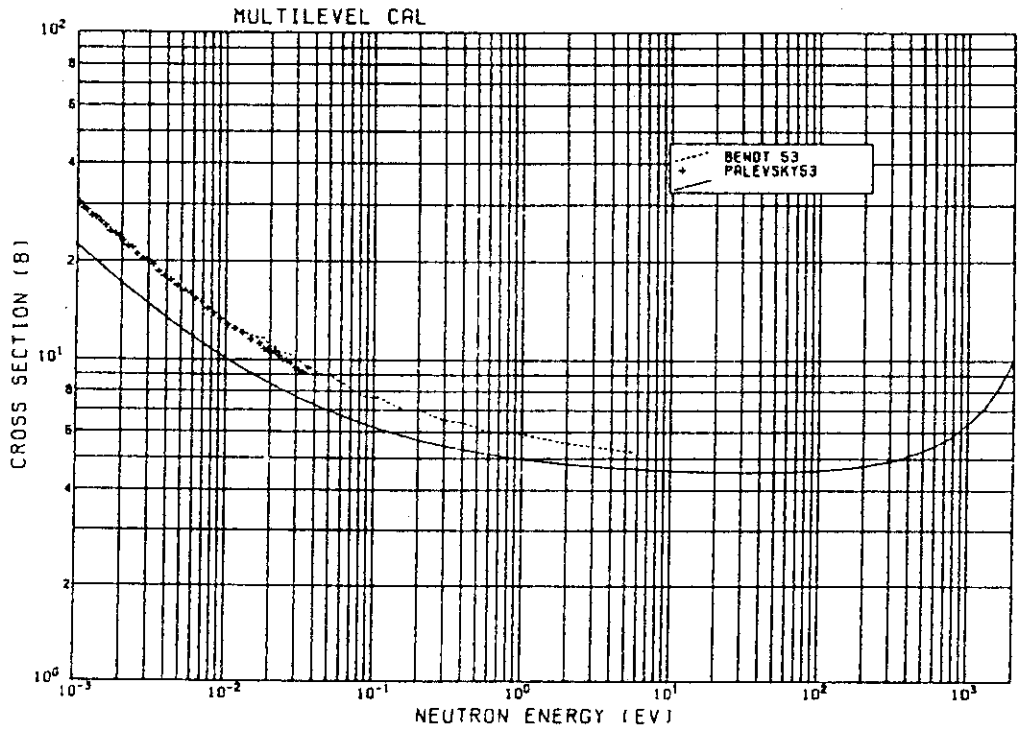


Fig. 1.1 Comparison of measured and calculated total cross sections of vanadium below keV region. The solid curve represents the calculated result as described in the text.

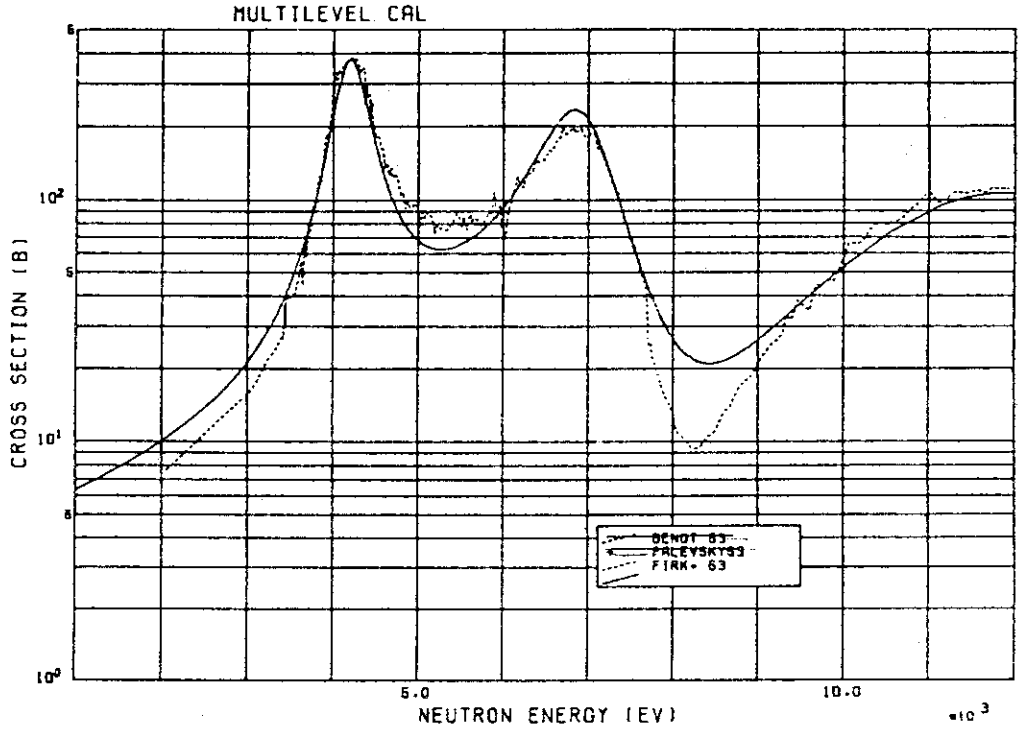


Fig. 1.2 Comparison of measured and calculated total cross sections of vanadium in the keV region. The solid curve represents the calculated result as described in the text.

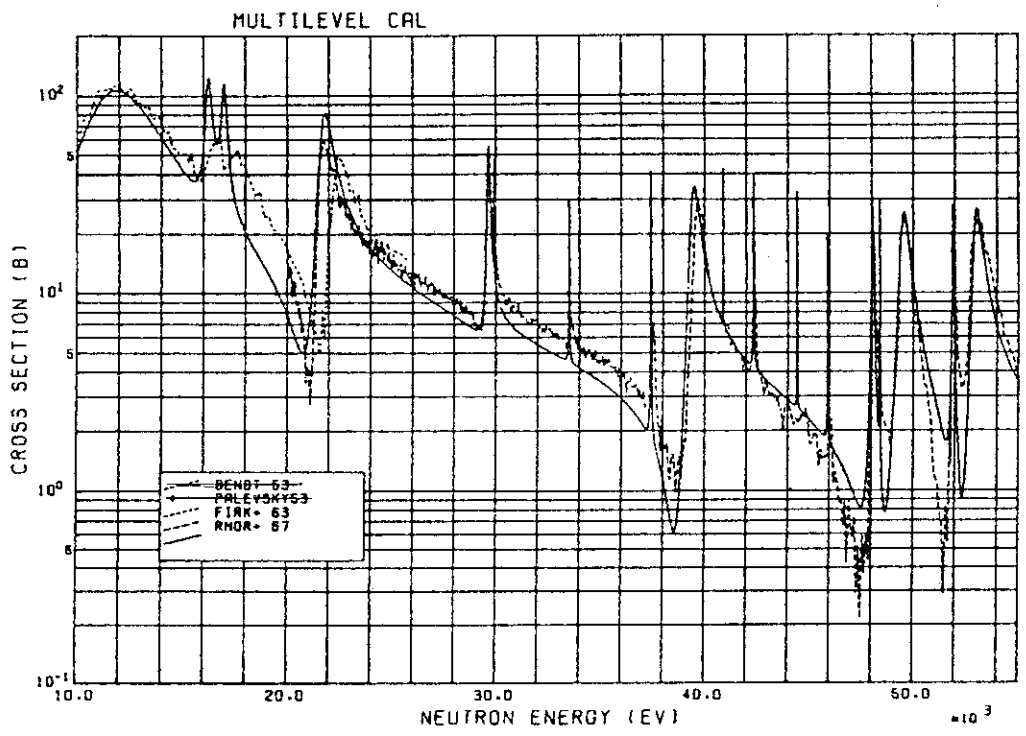


Fig. 1.3 Comparison of measured and calculated total cross sections of vanadium in the energy range 10 to 50 keV. The solid curve represents the calculated result as described in the text.

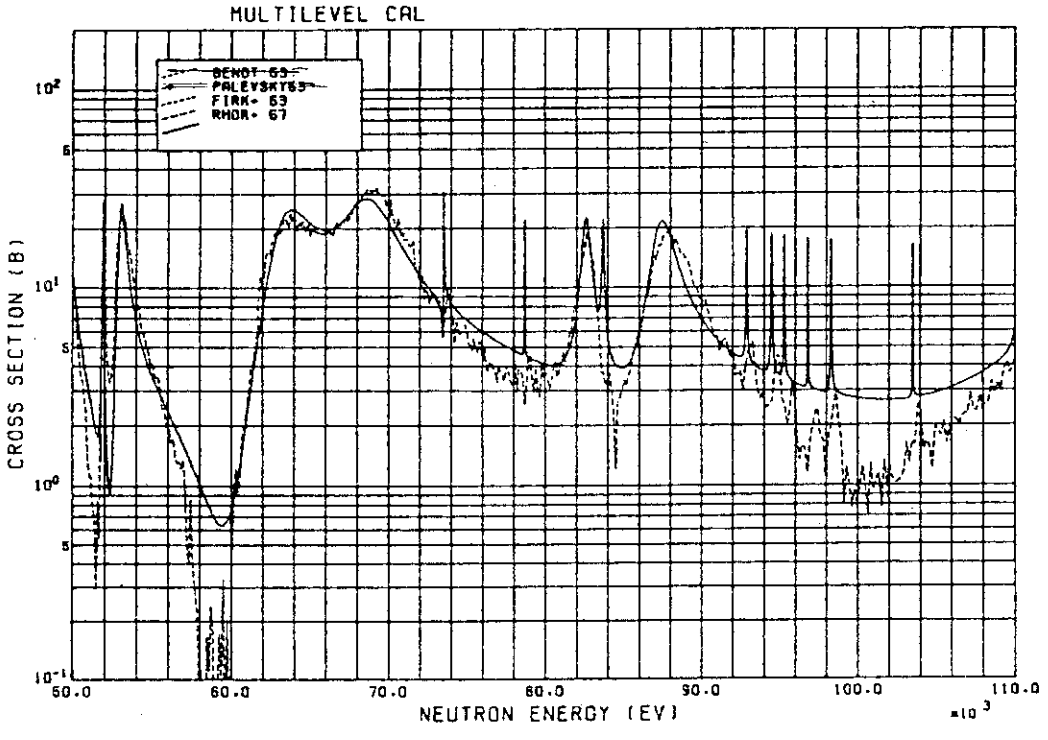


Fig. 1.4 Comparison of measured and calculated total cross sections of vanadium in the energy range 50 to 110 keV. The solid curve represents the calculated result as described in the text.

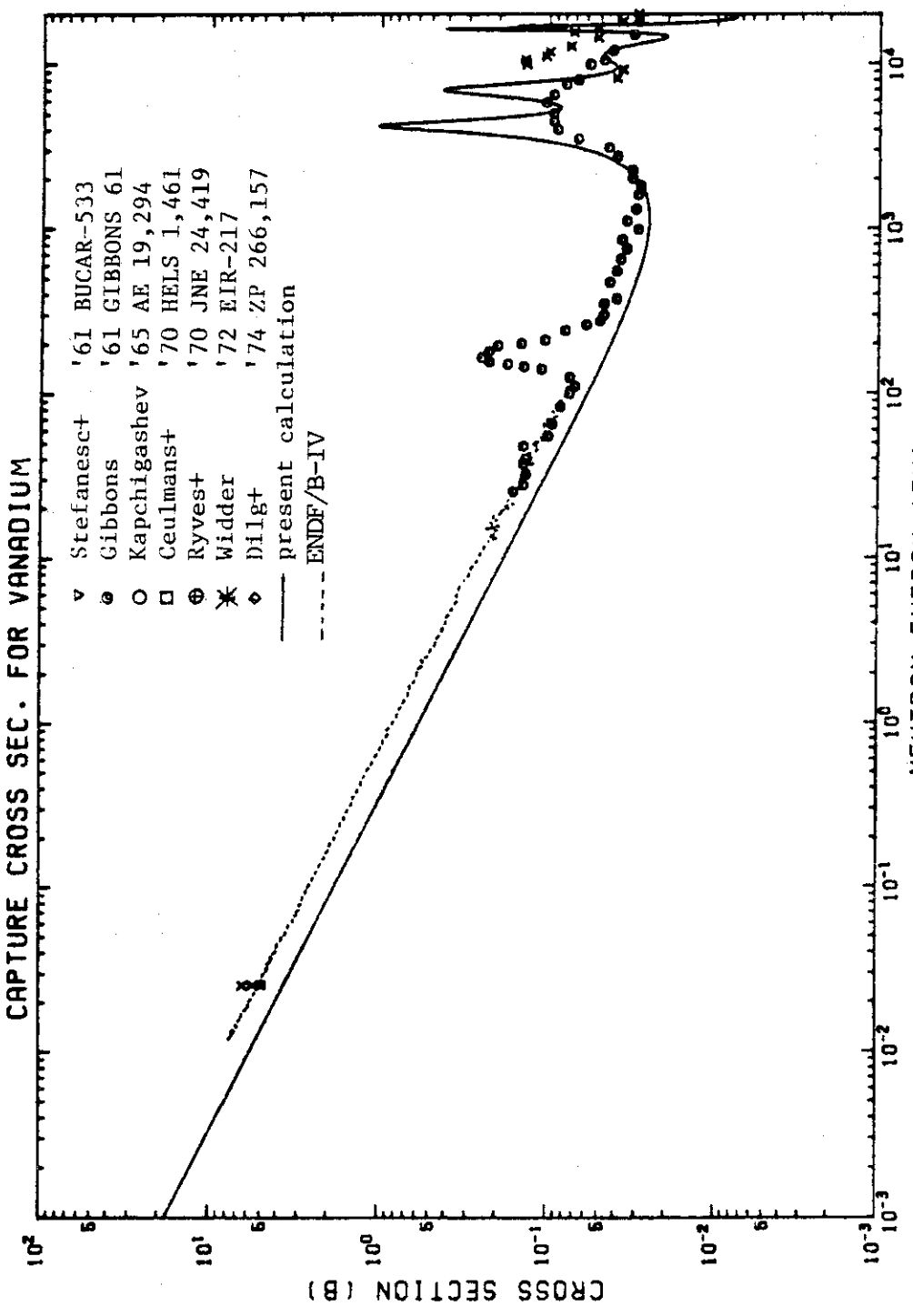


Fig. 2 Measured and calculated capture cross sections of vanadium up to 20 keV. The solid curve represents the present calculation for $^{51}V$ and the dashed curve the evaluated data of ENDF/B-IV for natural vanadium. The peak at 167 eV is due to the $^{50}V$ (abundance 0.24 %) in natural vanadium.

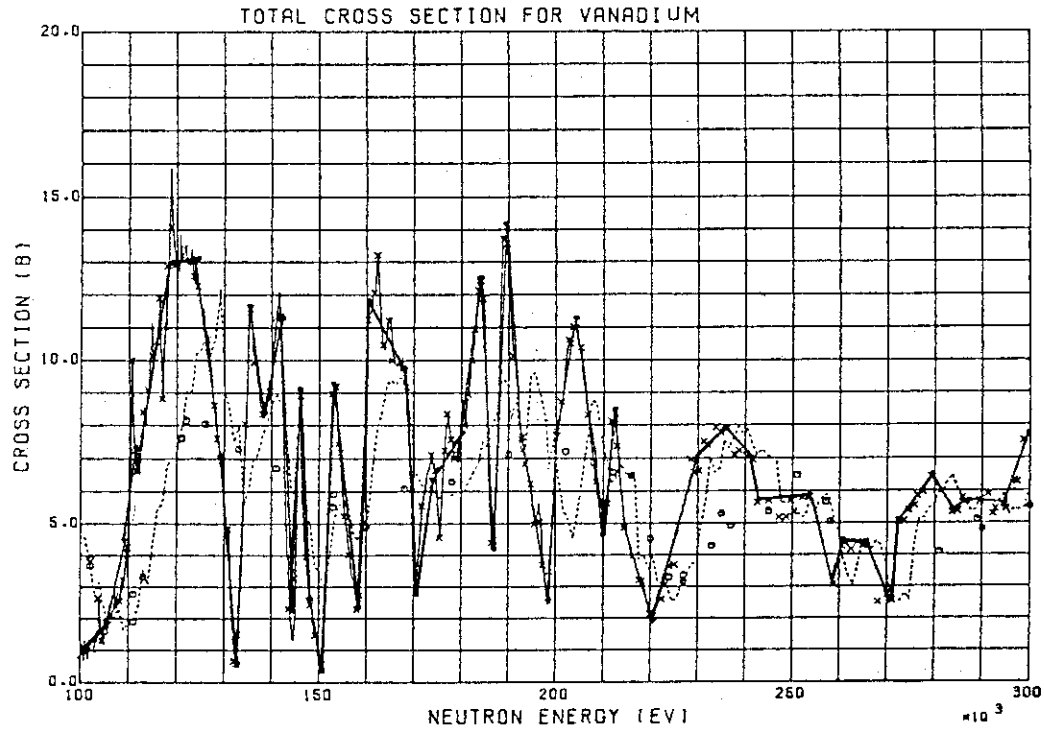


Fig. 3.1 Measured and evaluated total cross sections of vanadium in the energy range 100 to 300 keV. The thick lines show the evaluated values. Experimental values are referenced as follows: ——— = ref. 7), ---- = ref. 15) and ∘ = ref. 17).

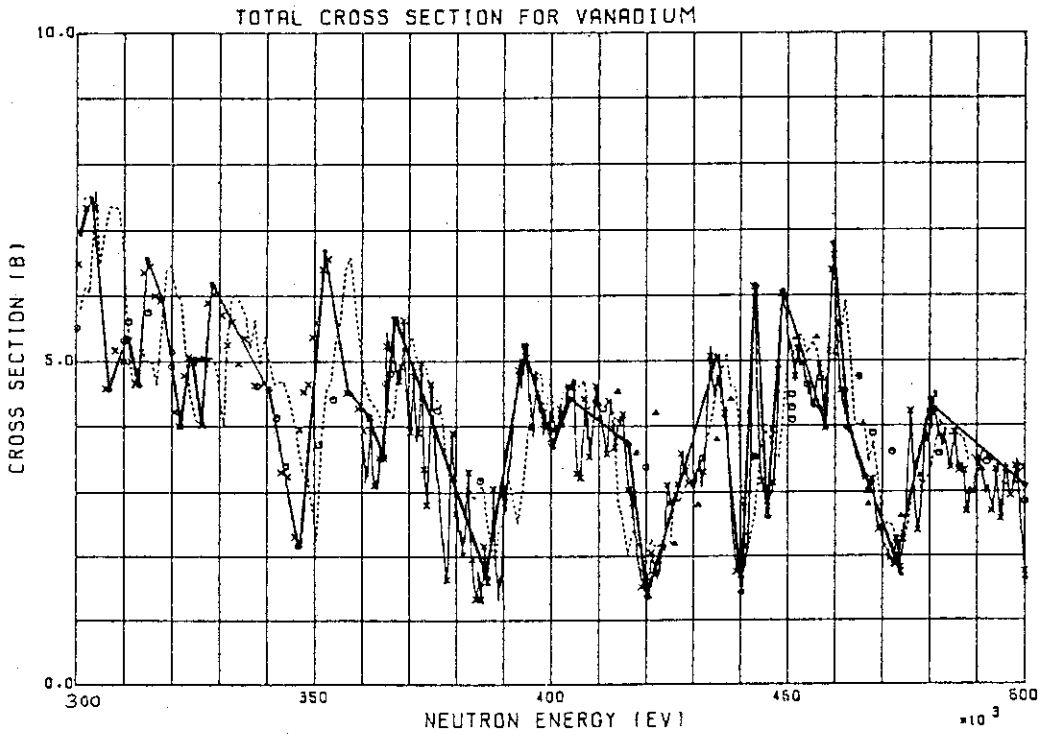


Fig. 3.2 Measured and evaluated total cross sections of vanadium in the energy range 300 to 500 keV. The thick lines show the evaluated values. Experimental values are referenced as follows: ---- = ref. 15), ——— = ref. 16), ∘ = ref. 17) and △ = ref.18).

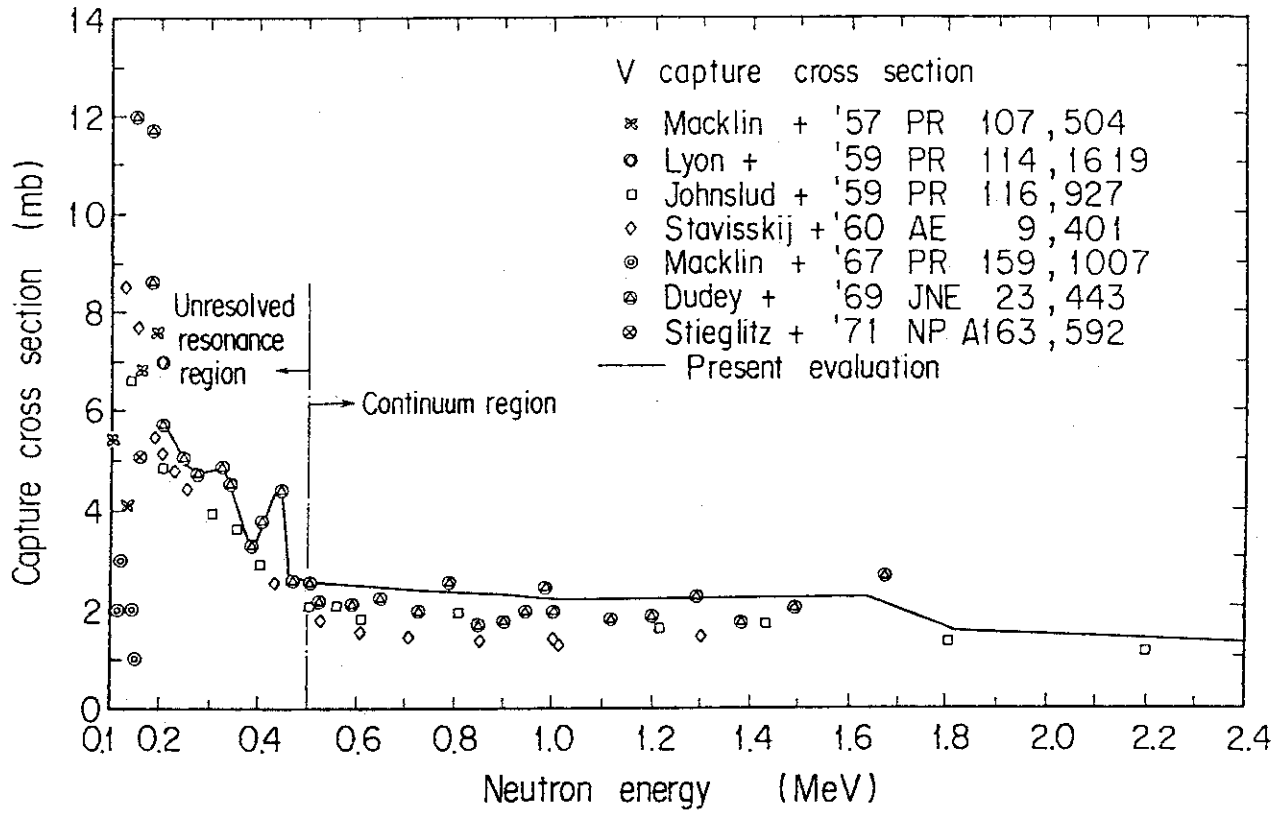


Fig.4 Comparison of measured and evaluated caprure cross sections of vanadium in the energy range 0.1 to 2.4 MeV. The solid curve is the present evaluation.

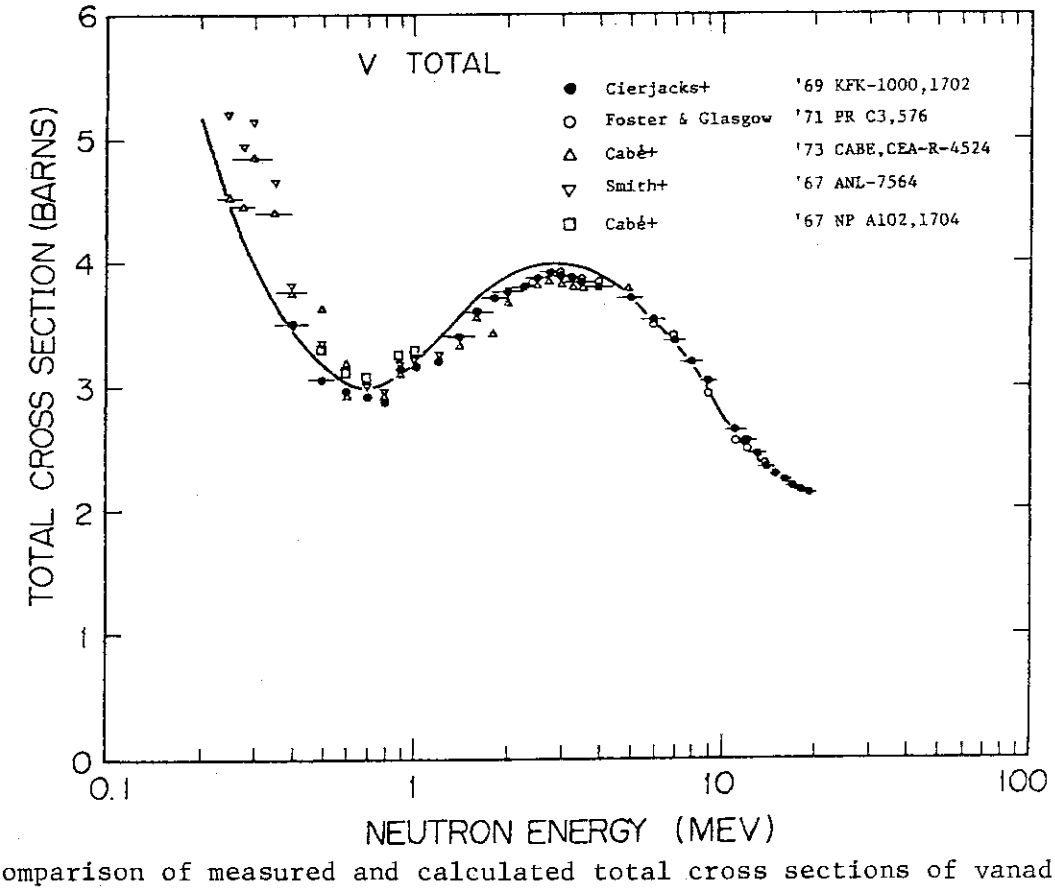


Fig.5 Comparison of measured and calculated total cross sections of vanadium. The solid curve represents the optical model calculation. For comparison, all of the measured values are those averaged within the energy intervals shown by horizontal bars for some typical data.

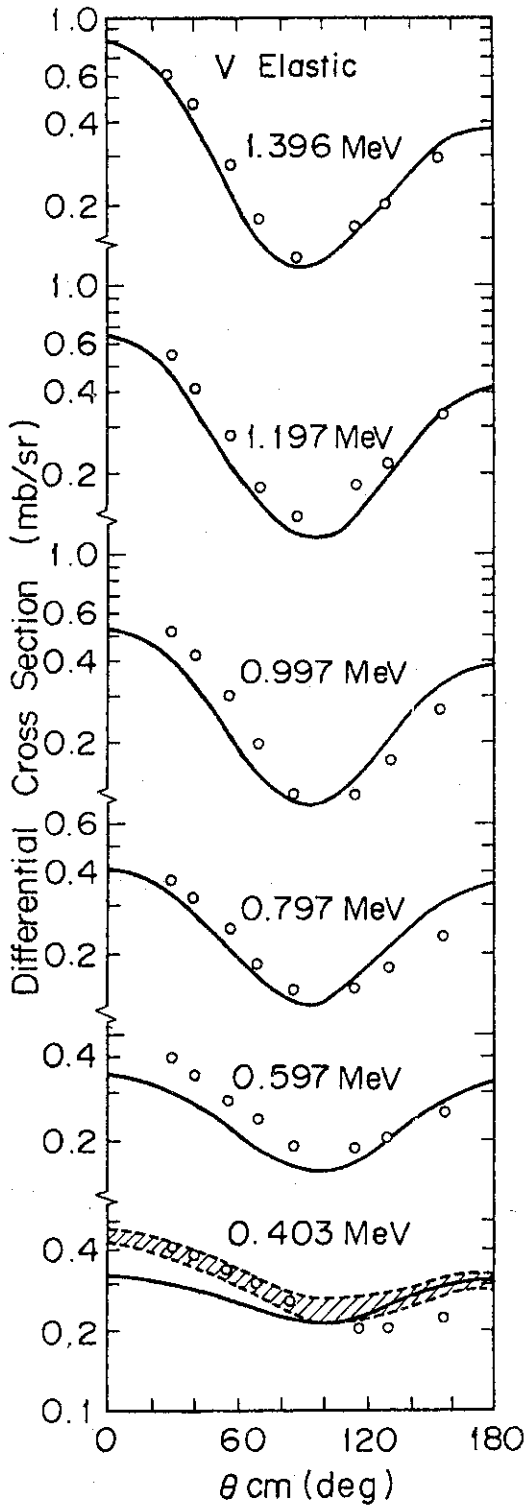


Fig. 6.1 Comparison of measured and calculated differential elastic scattering cross sections of vanadium. The solid curves represent the calculated results for the shape elastic plus compound elastic scattering. The measured cross sections denoted by open circles are the data of Smith et al.[15] The hatched area shows the range of uncertainty of the cross sections averaged over an energy interval of ± 100 keV.

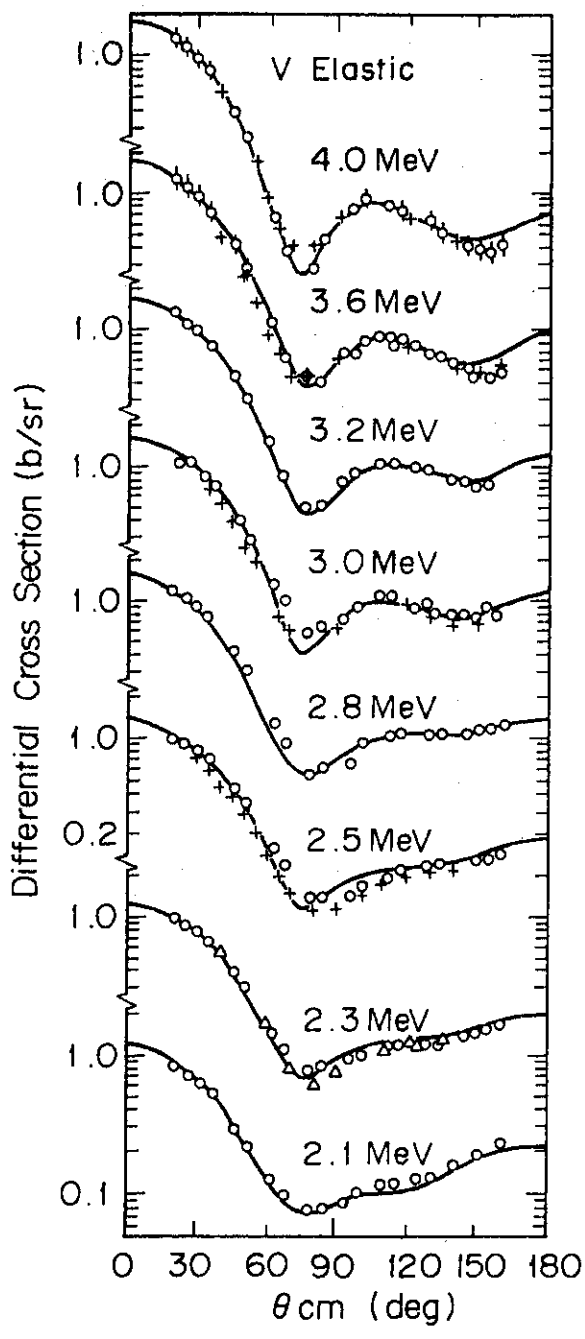


Fig. 6.2 Comparison of measured and calculated differential elastic scattering cross sections of vanadium. The solid curves represent the calculated results for the shape elastic plus compound elastic scattering. Experimental values are referenced as follows: ∘ = ref. 15), △= ref. 44) and + = ref. 45).

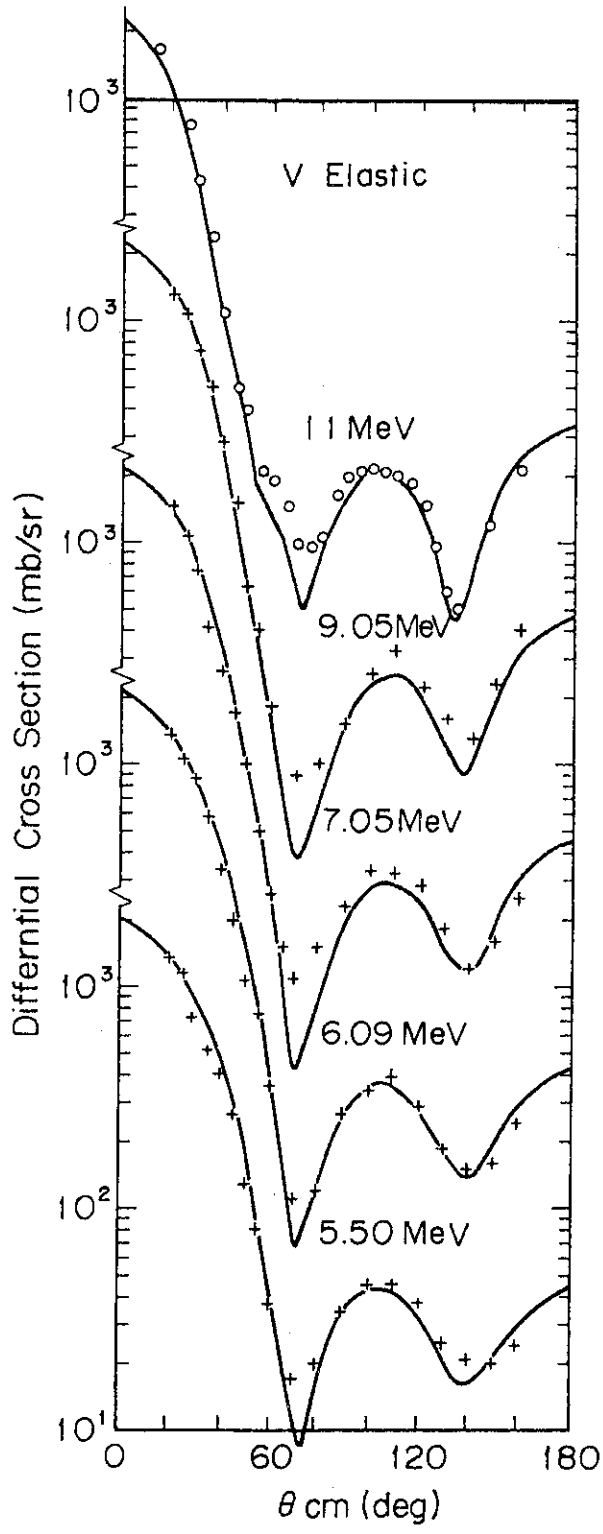


Fig. 6.3 Comparison of measured and calculated differential elastic scattering cross sections of vanadium. The solid curves represent the calculated results for the shape elastic scattering. Experimental values are referenced as follows: + = ref. 45) and ∘ = ref. 46).

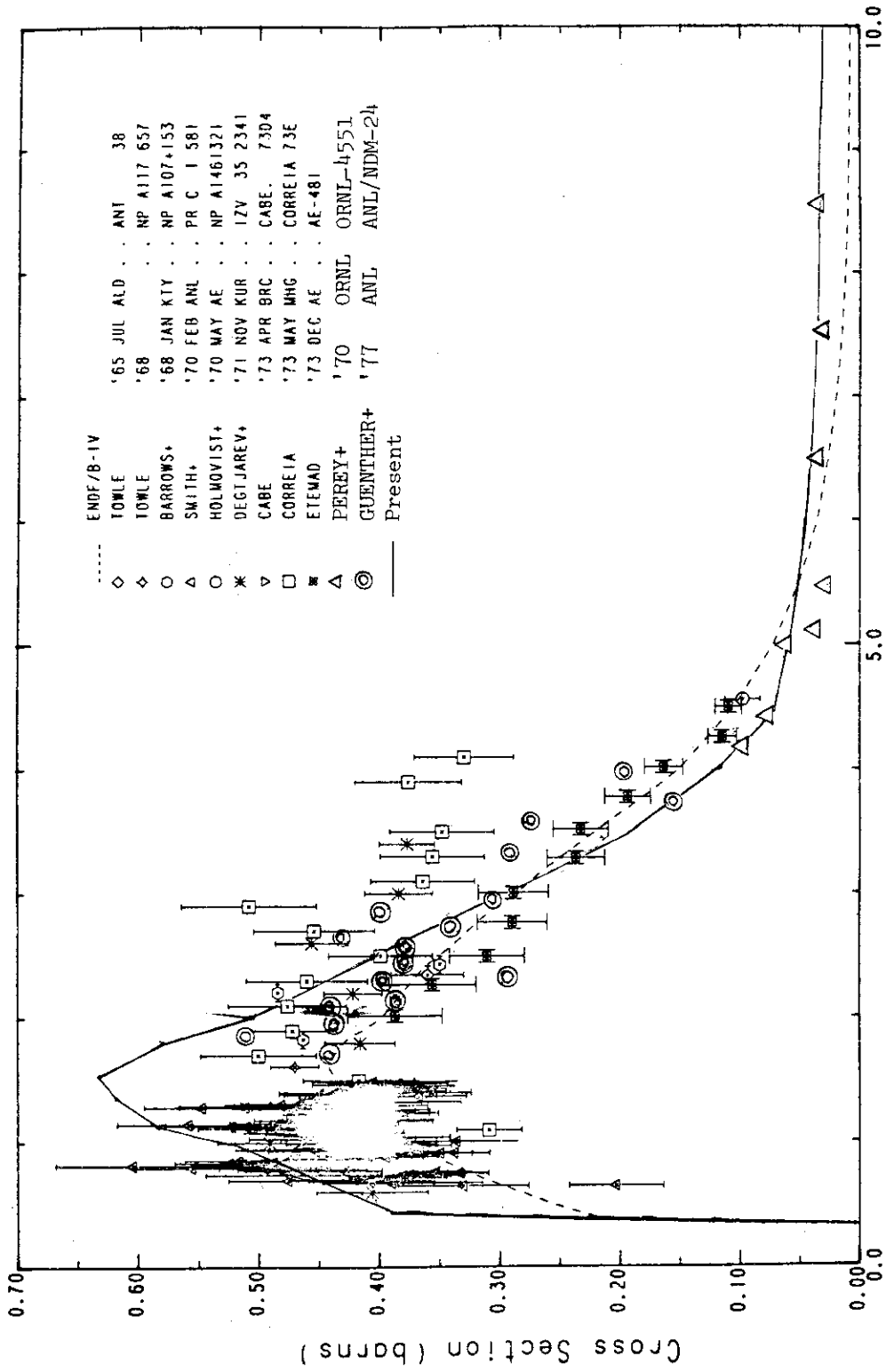


Fig. 7.1 Comparison of measured and evaluated inelastic scattering cross sections for 0.3201 MeV level. The solid curve represents the present evaluation and the dashed curve the evaluation of ENDF/B-IV[13].

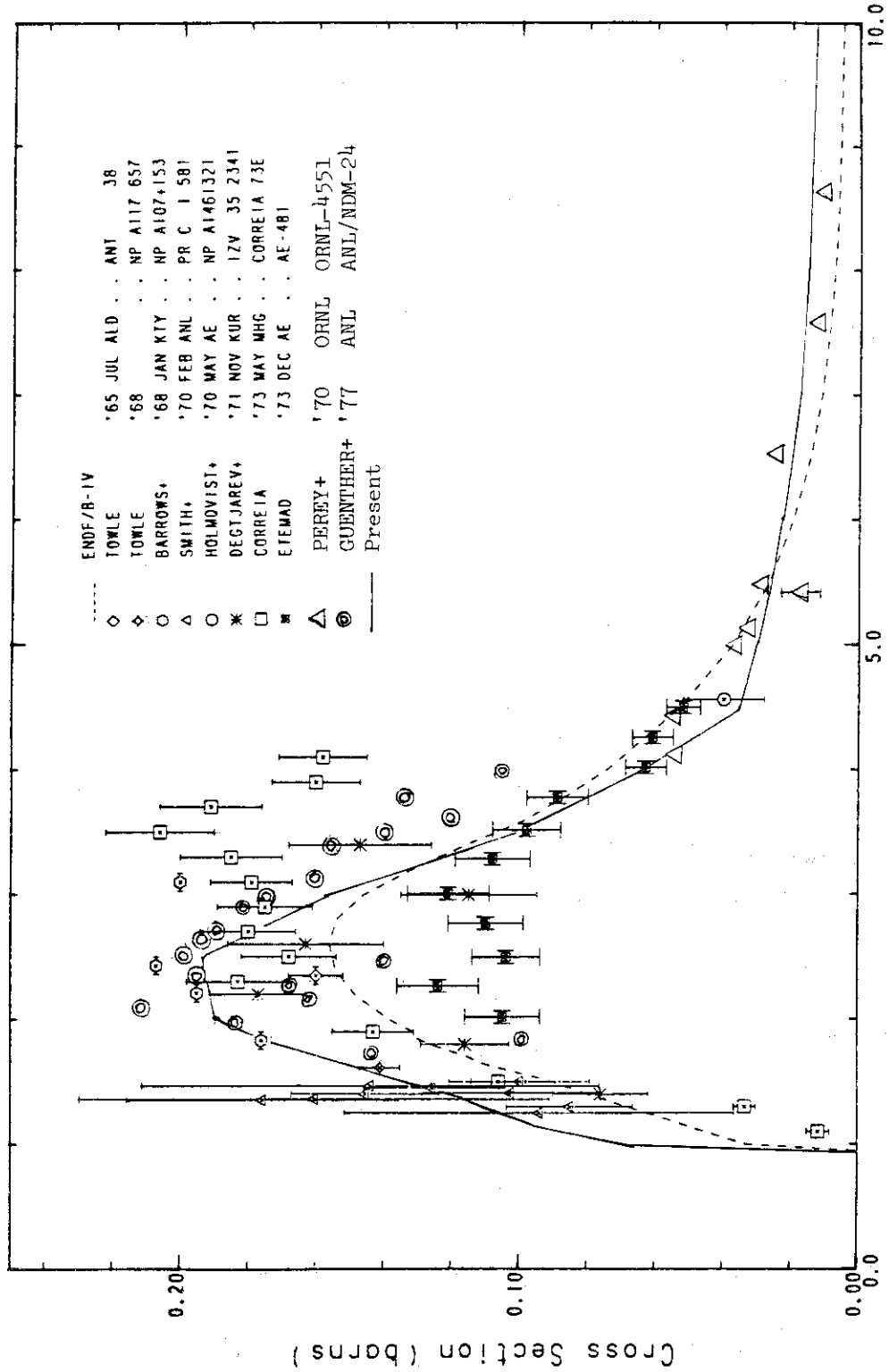


Fig. 7.2 Comparison of measured and evaluated inelastic scattering cross sections for the 0.9286 MeV level. The solid curve represents the present evaluation and the dashed curve the evaluation of ENDF/B-IV[13].

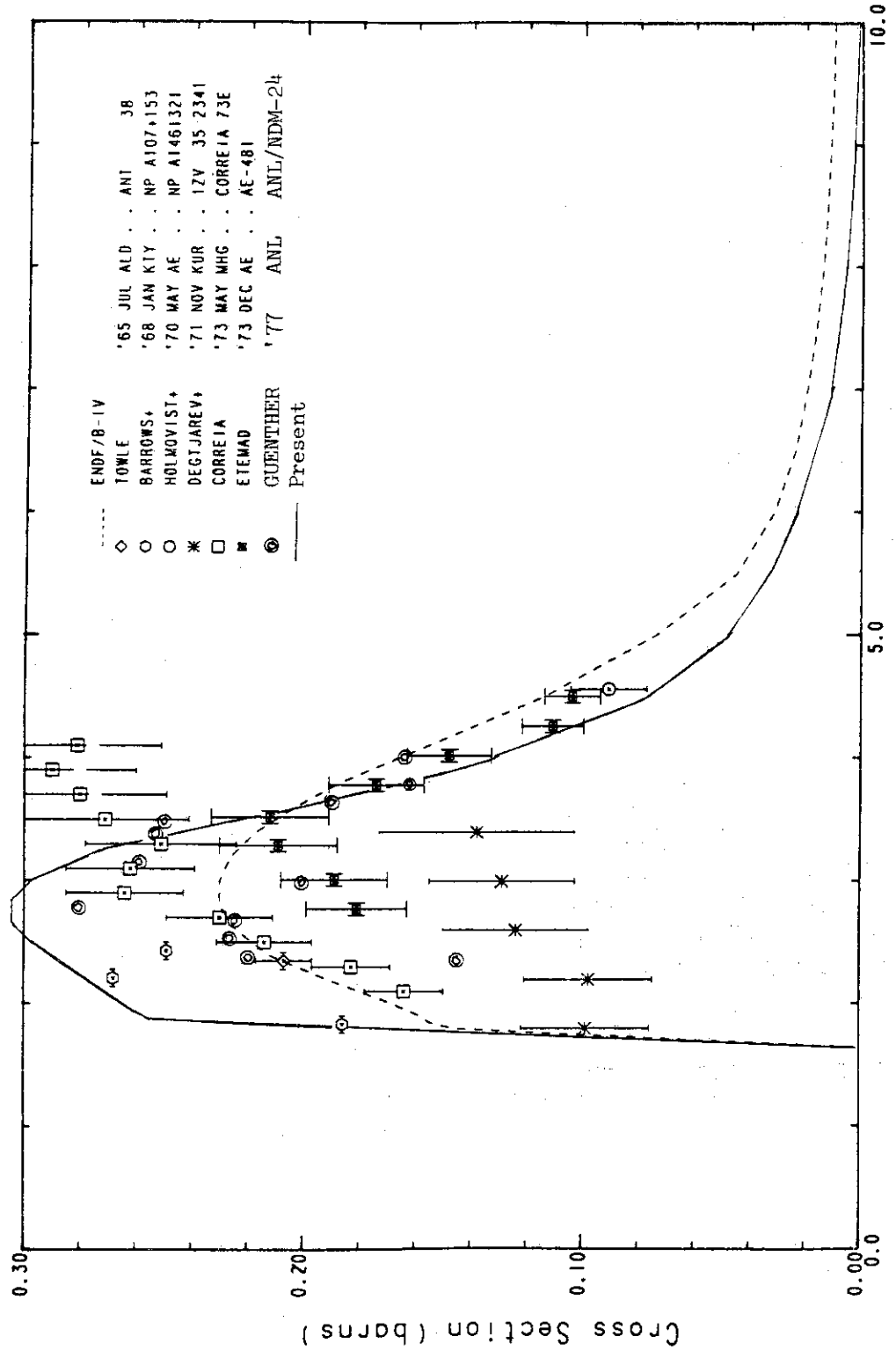


Fig. 7.3 Comparison of measured and evaluated inelastic scattering cross sections for the 1.6093 MeV level. The solid curve represents the present evaluation and the dashed curve the evaluation of ENDF/B-IV[13].

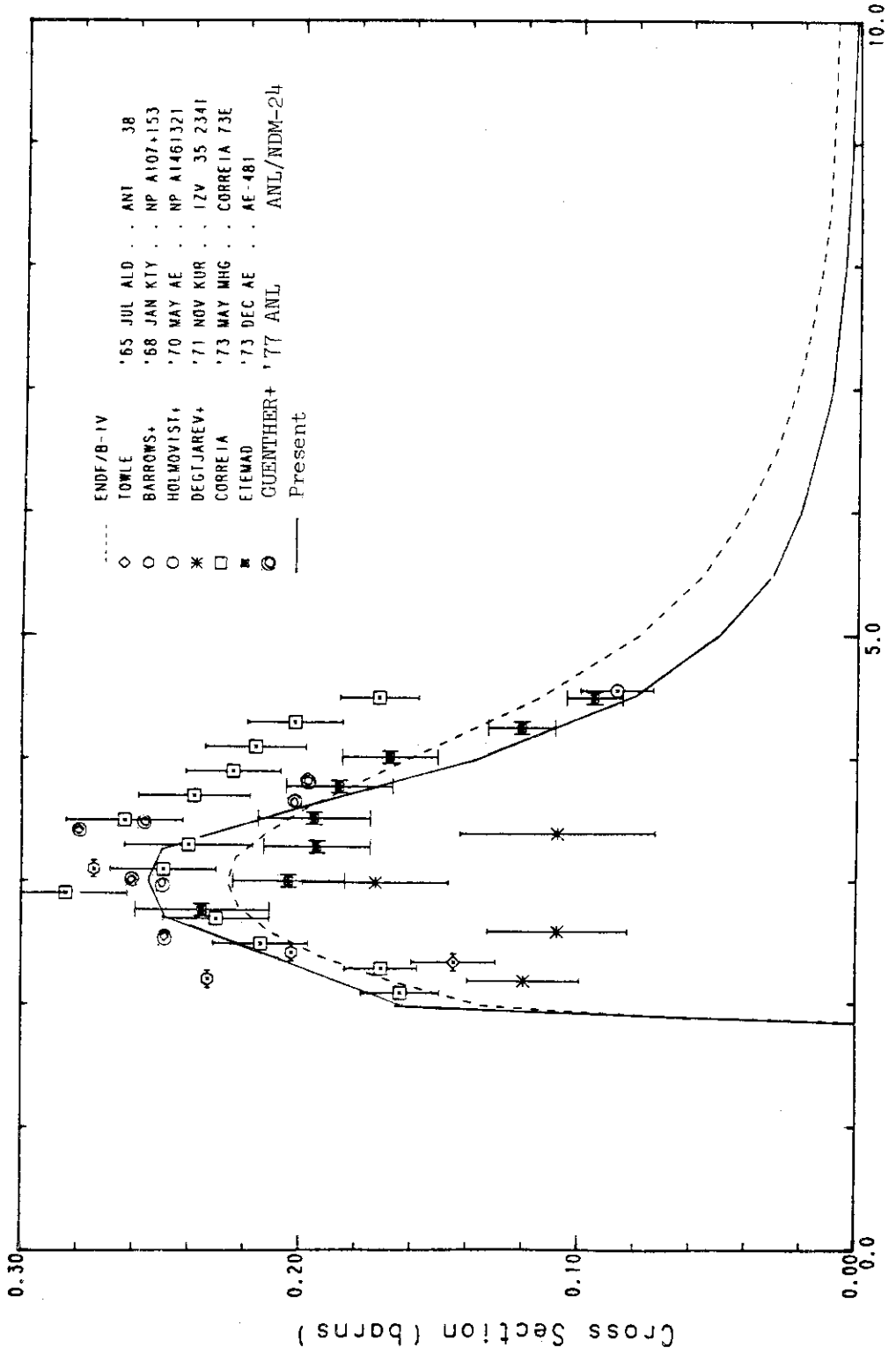


Fig. 7.4 Comparison of measured and evaluated inelastic scattering cross sections for the 1.8132 MeV level. The solid curve represents the present evaluation and the dashed curve the evaluation of ENDF/B-IV[13].

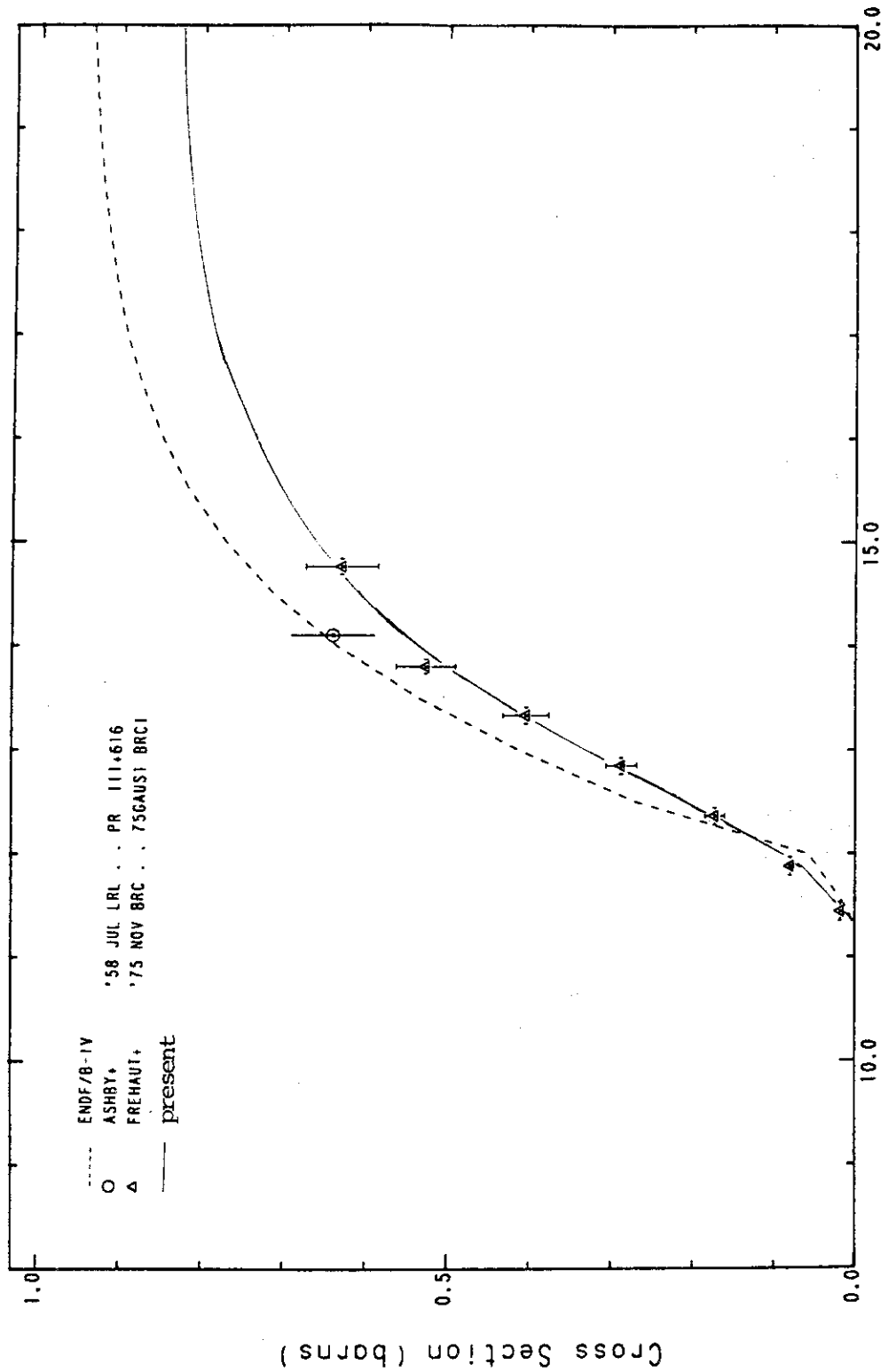


Fig. 8 Measured and evaluated (n,2n) reaction cross sections of vanadium. The solid curve indicates the present evaluation and the dashed curve the evaluation of ENDF/B-IV[13].

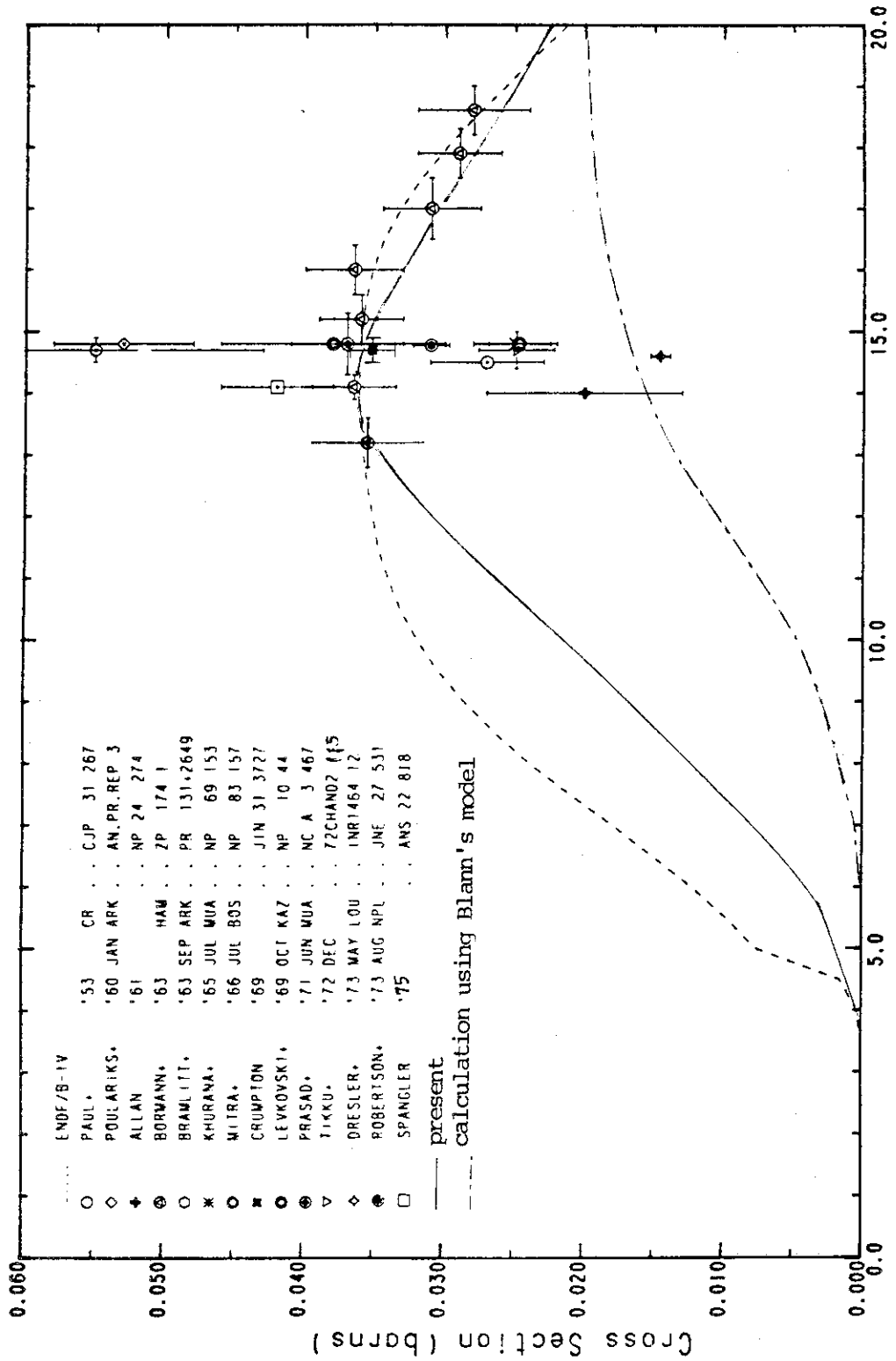


Fig. 9 Measured and evaluated (n,p) reaction cross sections of vanadium. The solid curve indicates the present evaluation, the dash-dot curve the result calculated by using Blann's hybrid model, and the dashed curve the evaluation of ENDF/B-IV[13].

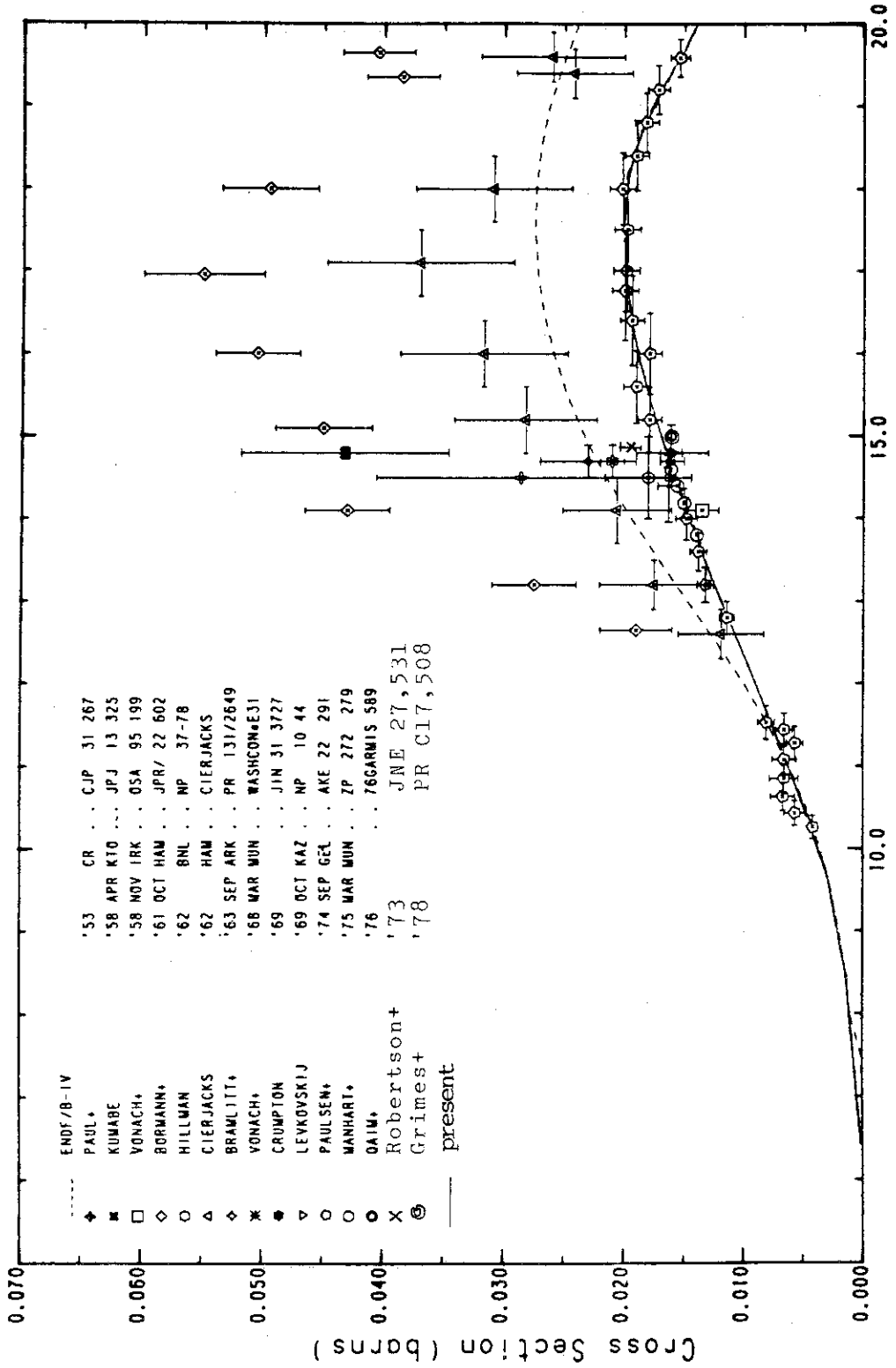


Fig. 10 Measured and evaluated (n,$\alpha$) reaction cross sections of vanadium. The solid curve indicates the present evaluation and the dashed curve the evaluation of ENDF/B-IV[13].

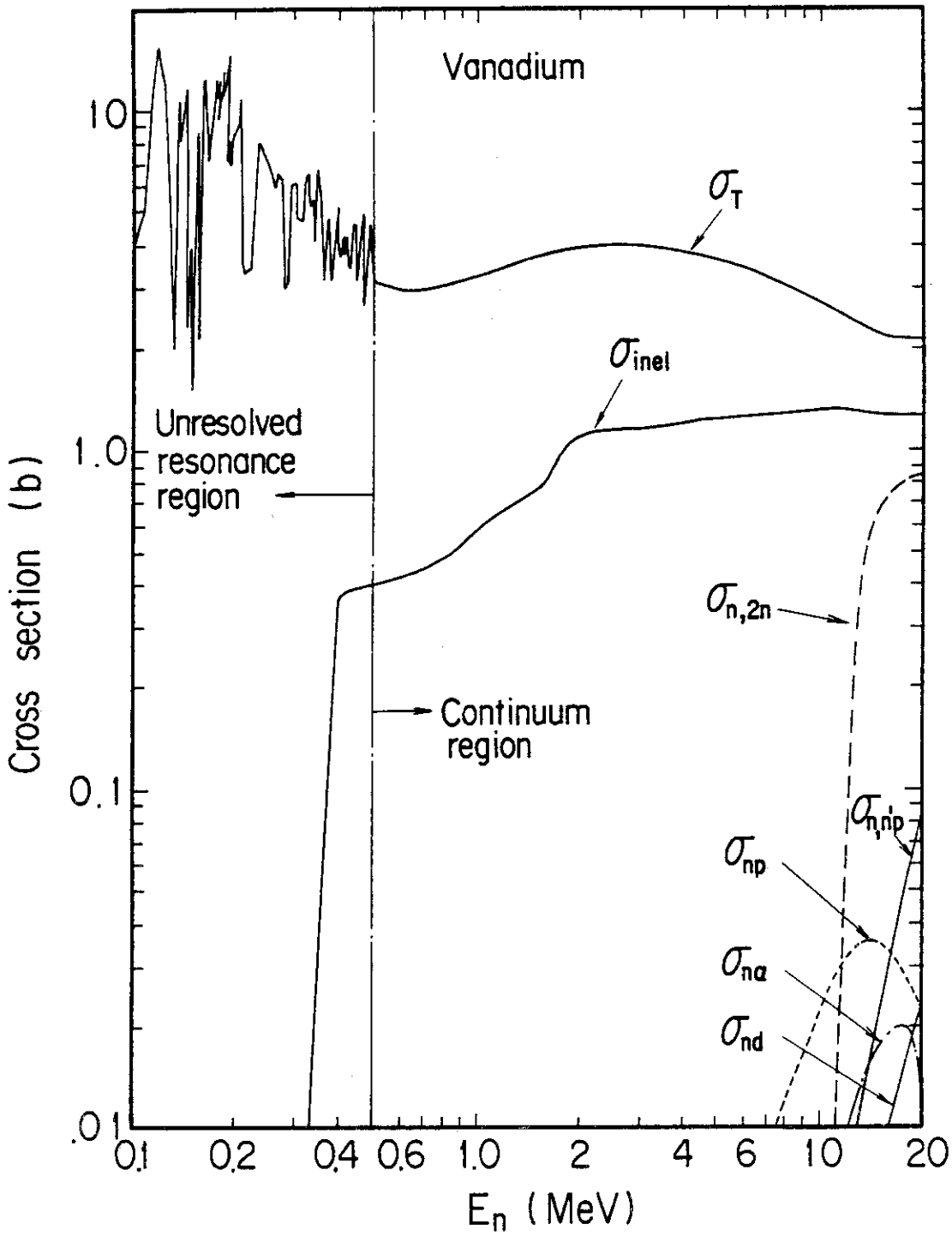


Fig. 11 Evaluated cross sections in the energy range above 100 keV. The capture cross sections are not shown in the figure, because most values of the cross sections are less than 0.01 barn.